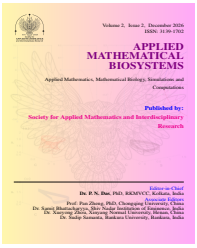
Applied Mathematical Biosystems, Volume 2, Issue 2, (Jul-Dec 2026), 71-86

Applied Mathematical Biosystems

journal homepage: https://ambjournal.com



Stability and Bifurcation Analysis of a Predator–Prey Model Using Carrying Capacity Variations

Boudhayan Bhattacharya[1] **and Phonindra Nath Das**[1]

[1]*Department of Mathematics, Ramakrishna Mission Vivekananda Centenary College, Rahara, Kolkata-700118, West Bengal, India*

Abstract

We propose and analyse a predator–prey model with prey group defence, non-linear Michaelis–Menten harvesting of the prey, and a dynamically varying carrying capacity. The carrying capacity follows a saturating shifted-logistic equation that stays between a positive minimum i and a maximum j. We prove non-negativity and boundedness of solutions, with forward uniqueness at prey extinction. We classify the predator-free equilibria at each capacity level, including the case of two coexisting predator-free states and their merger at a saddle-node. Among the equilibria, only those at the maximum capacity $K = j$ can be locally asymptotically stable, because $K = i$ is always repelling. Using Sotomayor's theorem, we prove two transcritical bifurcations, driven by the predator mortality rate and by the catchability coefficient, and a saddle-node bifurcation of the predator-free equilibria. We establish a Hopf-bifurcation at the coexistence equilibrium through eigenvalue crossing and transversality, and a numerically computed first Lyapunov coefficient shows that it is supercritical. We also derive an exact implicit solution and recovery time for the carrying capacity and prove that the recovery time increases strictly with the saturation parameter. Numerical simulations illustrate the results. In the parameter set studied, the group defence exponent has a non-monotonic effect on coexistence stability, whereas higher predator mortality is stabilising.

Keywords: *Prey-predator model; Variable carrying capacity; Group defence; Harvesting; Dynamical systems; Bifurcation*

Corresponding author: Phonindra Nath Das *E-mail address:* pdas@rkmvccrahara.ac.in
Received: July 30, 2026 **Revised:** November 12, 2026 **Accepted:** November 17, 2026 **Published:** November 19, 2026
© Jul-Dec 2026 Society for Applied Mathematics and Interdisciplinary Research **DOI:** 10.67029/j.amb.2026.0022.29
Article classification: Research Article; **MSC 2020: 92D25 · 34D20 · 37G10 · 37G15**

1. Introduction

Prey–predator dynamics constitute a foundational component of Mathematical Ecology and Mathematical Biology, providing insights into the interactions between prey, predators and their environment. These interactions influence population sizes, biomass and ecosystem productivity over time [1, 2], and can also drive evolutionary changes affecting survival and reproduction across generations [3]. Since the introduction of the classical Lotka–Volterra prey–predator model [4, 5], considerable attention has been given to incorporating additional ecological factors, such as environmental variability [6], prey refuge [7], and harvesting mechanisms [8], to obtain more realistic descriptions of population dynamics.

The carrying capacity of a species is such a fundamental ecological factor in the formulation of prey–predator models. It represents the maximum population size that an environment can sustainably support under available resources and habitat conditions. Classical models typically treat carrying capacity as constant. However this assumption is ill-suited for natural ecosystems where resource availability shifts with climatic fluctuations [9], habitat conditions [10], and other environmental disturbances. This has motivated models in which carrying capacity evolves dynamically [11].

Meyer and Ausubel [12] were the first to formalize this idea, proposing a logistic growth law for the carrying capacity itself

$$\frac{dK}{dt} = \alpha_k(K - k_1)\left(1 - \frac{K - k_1}{k_2}\right)$$

under which K rises sigmoidally from an initial level k_1 toward a final level $k_1 + k_2$. This however, captures an environment whose resource-supporting capacity adjusts internally in response to its own state rather than through unbounded logistic saturation alone.

We build on the Meyer–Ausubel formulation to address this. Their model bounds K between two fixed levels k_1 and $k_1 + k_2$, with $K = k_1$ itself being a minimum, but adjusts at a constant per-capita rate throughout. We instead let the rate of adjustment saturate as K grows, while retaining a strictly positive minimum i below which the carrying capacity cannot fall. Starting from the shifted logistic law

$$\frac{\mathrm{d}K}{\mathrm{d}t} = \rho_0(K - i)\left(1 - \frac{K - i}{j - i}\right), \qquad 0 < i < j,$$

whose linear growth term $\rho_0(K-i)$ assumes a constant per-capita rate of increase however close K already is to the equilibrium level j, we replace it with the saturating form

$$\rho_0(K-i) \longrightarrow \frac{\rho_0(K-i)}{1+K/l} = \frac{\rho\,(K-i)}{l+K}, \qquad \rho = \rho_0\, l,$$

so that

$$\frac{\mathrm{d}\,K}{\mathrm{d}\,t} = \frac{\rho(K-i)}{l+K}\left(1-\frac{K-i}{j-i}\right), \qquad 0<i<j, \tag{1}$$

where $j>0$ is the carrying-capacity equilibrium level; $i\in(0,j)$ is the minimum level below which the carrying capacity cannot fall, and $l>0$ is the half-saturation level that controls how quickly the adjustment rate saturates as K increases. The parameter $\rho_0>0$ is the intrinsic adjustment rate and $\rho=\rho_0 l$ is the maximal rate at which K can adjust, since $\rho(K-i)/(l+K)\to\rho$ as $K\to\infty$.

Equation (1) reduces to the shifted logistic law for sufficiently large l at fixed ρ_0,

$$\frac{1}{1+K/l} = 1-\frac{K}{l}+O(l^{-2}).$$

Then we obtain

$$K' = \rho_0(K-i)\left(1-\frac{K-i}{j-i}\right)+O(l^{-1}), \qquad l\to\infty.$$

We incorporate this variable carrying-capacity formulation into the predator–prey model of Kumar and Kharbanda [13], which employs a fixed carrying capacity together with Michaelis–Menten harvesting of the prey species and group defence,

$$\begin{aligned}\frac{dX}{dT} &= rX\left(1-\frac{X}{k}\right)-aX^{\alpha}Y-\frac{qEX}{mE+nX},\\ \frac{dY}{dT} &= -d_1Y+aeX^{\alpha}Y.\end{aligned}$$

subject to $X(0)>0$, $Y(0)>0$. Here X and Y denote the prey and predator densities at time T, respectively. The parameter r is the intrinsic growth rate of the prey and k is the fixed carrying capacity; a is the search efficiency of predator for prey, with $\alpha\in(0,1]$ being the group defence; d_1 is the death rate of the predator; e is the conversion efficiency with which consumed prey biomass is converted into predator biomass; q is the catchability coefficient; E is the harvesting effort; and m,n are suitable constants governing the Michaelis–Menten harvesting term $\dfrac{qEX}{mE+nX}$, through which prey are harvested at a rate that saturates rather than growing unboundedly with effort E.

The paper is organised as follows. We first present the proposed model and its mathematical analysis, including the local stability of the equilibrium points and the associated bifurcations, followed by numerical simulations illustrating the theoretical results and the influence of key model parameters on the system dynamics, and finally conclude with a discussion of the main results.

2. Model

Suppose $N=N(t)$, $P=P(t)$ and $K=K(t)$ denote the prey population, predator population and environmental carrying capacity at time t, respectively. The parameter r represents the intrinsic growth rate of the prey population, a is the search efficiency of the predator for prey, $\alpha\in(0,1]$ is the group defence exponent of the prey population, e is the conversion efficiency with which consumed prey biomass is converted into predator biomass, d_1 denotes the mortality rate of the predator population, q is the catchability coefficient, E is the harvesting effort, and m,n are suitable constants governing the Michaelis–Menten harvesting term, which acts on the prey population. The carrying capacity K evolves according to equation (1), where j is its equilibrium capacity level, $i\in(0,j)$ is its minimum level, and $l>0$ is the half-saturation level of its adjustment rate. The parameter $\rho_0>0$ is the intrinsic adjustment rate and $\rho=\rho_0\,l$ is the maximal rate at which K can adjust. Thus our model is given by,

$$\begin{aligned}\frac{dN}{dt} &= rN\left(1-\frac{N}{K}\right)-aN^{\alpha}P-\frac{qEN}{mE+nN},\\ \frac{dP}{dt} &= -d_1P+aeN^{\alpha}P,\\ \frac{dK}{dt} &= \frac{\rho\,(K-i)}{l+K}\left(1-\frac{K-i}{j-i}\right)=\frac{\rho_0\,(K-i)}{1+K/l}\left(1-\frac{K-i}{j-i}\right),\\ &\qquad 0<i<j,\ \rho=\rho_0\,l.\end{aligned} \tag{2}$$

where all the parameters are positive, and $N(0)>0$, $P(0)>0$, $i\le K(0)\le j$ are the initial conditions.

3. Theoretical analysis

The term $aN^{\alpha}P$ in (2), for $\alpha\in(0,1)$, is not locally Lipschitz continuous at $N=0$, because $\partial_N N^{\alpha}\to\infty$ as $N\to0^{+}$. Hence the Picard–Lindelöf theorem does not apply at points with $N=0$ and $P>0$, and it cannot be used there to conclude uniqueness. Forward uniqueness nevertheless holds, because $N=0$ is invariant and $N(t_0)=0$ forces $N(t)=0$ for all $t\ge t_0$. Uniqueness backward in time can fail at $N=0$. Moreover N^{α} is defined only for $N\ge0$, and orbits that start near the origin above a certain separatrix can reach $N=0$ in finite time [14]. Strict positivity of N therefore cannot hold in general, and solutions are considered on forward intervals only.

Let $N_{+}=\max\{N,0\}$ and consider the extended system

$$\begin{aligned}\frac{dN}{dt} &= rN_{+}\left(1-\frac{N_{+}}{K}\right)-aN_{+}^{\alpha}P-\frac{qEN_{+}}{mE+nN_{+}},\\ \frac{dP}{dt} &= -d_1P+aeN_{+}^{\alpha}P,\\ \frac{dK}{dt} &= \frac{\rho\,(K-i)(j-K)}{(l+K)(j-i)}.\end{aligned} \tag{3}$$

This system is defined for all real N and P and for $K>0$, it coincides with (2) when $N\ge0$, and the right-hand side of its first equation vanishes when $N<0$. A solution of (3) on $[0,T)$, where $0<T\le\infty$, is a continuously differentiable map from $[0,T)$ into $\mathbb{R}^2\times(0,\infty)$ that satisfies (3) at every point of $[0,T)$. A solution of (2) on $[0,T)$ is a continuously differentiable map from $[0,T)$ into $[0,\infty)\times\mathbb{R}\times(0,\infty)$ that satisfies (2) at every point of $[0,T)$. A solution on $[0,T)$ is maximal if there is no solution on an interval $[0,\widetilde{T})$ with $\widetilde{T}>T$ that coincides with it on $[0,T)$. The proof below also shows that two solutions with the same initial value coincide on their common interval of existence, and that a solution with $N(t_0)=0$ satisfies $N(t)=0$ and $P(t)=P(t_0)e^{-d_1(t-t_0)}$ for all later times $t\ge t_0$.

Theorem 3.1. *Let $\alpha\in(0,1]$, $N_0\ge0$, $P_0\ge0$ and $K_0\in[i,j]$. Then system (3) has a solution with initial value (N_0,P_0,K_0) defined on $[0,\infty)$, and every solution of system (3) with this initial value satisfies $N(t)\ge0$, $P(t)\ge0$ and $i\le K(t)\le j$ on its interval of existence. In particular, the set $\mathcal{R}=\mathbb{R}^2_{+}\times[i,j]$ is positively invariant for (2).*

Proof. The third equation of (3) does not involve N and P. Its right-hand side

$$H(K) = \frac{\rho\,(K-i)(j-K)}{(l+K)(j-i)}$$

is continuously differentiable on $(-l,\infty)$, which contains $[i,j]$. Hence for each $K_0 \in [i,j]$ this equation has exactly one maximal solution K. Since $H(i) = H(j) = 0$, the constant functions equal to i and to j are solutions, and so K is constant if $K_0 = i$ or $K_0 = j$. Let $K_0 \in (i,j)$. If $K(t_*) = i$ or $K(t_*) = j$ at some t_* in the interval of existence, then uniqueness shows that K coincides with a constant solution, which contradicts $K_0 \in (i,j)$. Therefore $i < K(t) < j$ on the interval of existence. A solution that remains in the compact interval $[i,j]$ can be continued to $[0,\infty)$. Thus in every case K is defined on $[0,\infty)$, is continuously differentiable, and satisfies $i \le K(t) \le j$ for all $t \ge 0$. The third component of every solution of (3) and of every solution of (2) with initial value K_0 is the restriction of this function to the interval of existence. Consequently (N,P,K) is a solution of (3) if and only if (N,P) solves the first two equations of (3) with K replaced by the function $K(t)$.

Since $K(t) \ge i > 0$ and $mE + nN_+ \ge mE > 0$, the right-hand sides of the first two equations of (3) with K replaced by $K(t)$ are continuous in $(t,N,P) \in [0,\infty)\times\mathbb{R}^2$. By Peano's existence theorem there is a solution of these two equations for every initial value, and every solution can be continued to a maximal solution. By the continuation theorem for ordinary differential equations with continuous right-hand side, a maximal solution defined on an interval $[0,T)$ with $T < \infty$ is unbounded.

Let (N,P,K) be a solution of (3) on an interval $[0,T)$ with initial value (N_0,P_0,K_0). Put $k(t) = -d_1 + aeN_+(t)^\alpha$. The function k is continuous and the second equation reads $P' = kP$. Hence the function $P(t)\exp\bigl(-\int_0^t k(s)\,ds\bigr)$ has derivative zero, and

$$P(t) = P_0 \exp\Bigl(\int_0^t k(s)\,ds\Bigr)$$

for all $t \in [0,T)$. Since $P_0 \ge 0$, it follows that $P(t) \ge 0$ for all $t \in [0,T)$, and $P(t) = 0$ for all $t \in [0,T)$ if $P_0 = 0$.

Suppose that $N(t_1) < 0$ for some $t_1 \in (0,T)$. The set of all $t \in [0,t_1]$ with $N(t) \ge 0$ is closed and contains 0, so it has a largest element t_0. Then $t_0 < t_1$ and $N(t) < 0$ for all $t \in (t_0,t_1]$, and the continuity of N gives $N(t_0) = 0$. If $N < 0$, then $N_+ = 0$ and the right-hand side of the first equation equals zero. Hence $N'(t) = 0$ for all $t \in (t_0,t_1]$, so N is constant on $[t_0,t_1]$ and $N(t_1) = N(t_0) = 0$. This contradicts $N(t_1) < 0$. Therefore $N(t) \ge 0$ for all $t \in [0,T)$. Consequently $N_+ = N$ along the solution.

Let (N,P,K) be a maximal solution of (3) with initial value (N_0,P_0,K_0) on $[0,T)$ and suppose that $T < \infty$. Since $N \ge 0$, $P \ge 0$ and $0 < K \le j$ on $[0,T)$, the first equation gives

$$\frac{dN}{dt} \le rN\Bigl(1-\frac{N}{K}\Bigr) \le rN\Bigl(1-\frac{N}{j}\Bigr),$$

and the right-hand side is negative whenever $N > j$. Put $\bar N = \max\{N_0, j\}$ and suppose that $N(t_1) > \bar N$ for some $t_1 \in (0,T)$. Let s be the largest $t \in [0,t_1]$ with $N(t) \le \bar N$. Then $N(s) = \bar N$ and $N(t) > \bar N \ge j$ for all $t \in (s,t_1]$, so $N' < 0$ on $(s,t_1]$ and $N(t_1) < N(s) = \bar N$, which is a contradiction. Hence $N(t) \le \bar N$ on $[0,T)$. The second equation now gives $P' \le ae\bar N^\alpha P$, and therefore $P(t) \le P_0 e^{ae\bar N^\alpha T}$ on $[0,T)$. Thus (N,P,K) is bounded on $[0,T)$, which contradicts the unboundedness of a maximal solution on a bounded interval. Hence $T = \infty$, and the maximal solution is defined on $[0,\infty)$.

Since $N \ge 0$, $P \ge 0$ and $K > 0$ along any solution of (3), the first equation gives

$$\frac{dN}{dt} = rN - \frac{rN^2}{K} - aN^\alpha P - \frac{qEN}{mE+nN} \le rN.$$

Hence $e^{-rt}N(t)$ is non-increasing, because its derivative equals $e^{-rt}(N' - rN) \le 0$. If $N(t_0) = 0$, then $0 \le e^{-rt}N(t) \le e^{-rt_0}N(t_0) = 0$ for all $t \ge t_0$ in the interval of existence, and so $N(t) = 0$ for all such t. The second equation then reduces to $P' = -d_1P$, and therefore $P(t) = P(t_0)e^{-d_1(t-t_0)}$ for all $t \ge t_0$.

Let (N_1,P_1,K) and (N_2,P_2,K) be solutions of (3) with the same initial value, and let $[0,T)$ be the intersection of their intervals of existence. Suppose that (N_1,P_1) and (N_2,P_2) differ at some point $t' \in [0,T)$. Let t_* be the supremum of all $t \in [0,T)$ such that the two solutions coincide on $[0,t]$. Then $t_* \le t' < T$, and by continuity the two solutions coincide on $[0,t_*]$. Let (N_*,P_*) be their common value at t_*. Suppose first that $N_* > 0$. Then $N_1 > 0$ and $N_2 > 0$ on a neighbourhood of t_* in $[0,T)$. On the region where $N > 0$ the right-hand sides of the first two equations, with K replaced by $K(t)$, are continuously differentiable with respect to (N,P) and their partial derivatives are continuous in (t,N,P). They are therefore locally Lipschitz continuous with respect to (N,P), and the Picard–Lindelöf theorem shows that the two solutions coincide on a right neighbourhood of t_* in $[0,T)$. This contradicts the definition of t_*. Suppose next that $N_* = 0$. By the previous paragraph $N_1(t) = N_2(t) = 0$ and $P_1(t) = P_2(t) = P_*e^{-d_1(t-t_*)}$ for all $t \in [t_*,T)$. Hence the two solutions coincide on all of $[0,T)$, which contradicts $t' \in [0,T)$. Therefore any two solutions with the same initial value coincide on the intersection of their intervals of existence.

Every solution of (2) takes values in $[0,\infty)\times\mathbb{R}\times(0,\infty)$, so $N_+ = N$ along it and it is also a solution of (3). Hence every solution of (2) with initial value in $\mathcal{R}$ satisfies $N(t) \ge 0$, $P(t) \ge 0$ and $i \le K(t) \le j$ on its interval of existence. Along the maximal solution of (3) defined on $[0,\infty)$ we have $N_+ = N$, so this solution is a solution of (2) on $[0,\infty)$ with values in $\mathcal{R}$. Therefore $\mathcal{R}$ is positively invariant for (2). □

Lemma 1. *For $N \ge 0$ and $K \in [i,j]$, the following inequality holds.*

$$N\Bigl(1-\frac{N}{K}\Bigr) \le \frac{K}{4} \le \frac{j}{4}.$$

Proof. Fix $K > 0$ and set $\varphi(N) = N - N^2/K$. Then $\varphi'(N) = 1 - 2N/K$ and $\varphi''(N) = -2/K < 0$, so φ is concave with a unique maximum at $N = K/2$, where $\varphi(K/2) = K/4$. Hence $\varphi(N) \le K/4$ for all $N \ge 0$. Since $K \le j$, it follows that $K/4 \le j/4$. □

Theorem 3.2. *Every solution of system (2) with initial conditions in $\mathcal{R}$ is bounded on its interval of existence.*

Proof. By Theorem 3.1, $N(t) \ge 0$, $P(t) \ge 0$, and $i \le K(t) \le j$ throughout the interval of existence, and the argument below uses only these non-negativity and upper-range facts rather than the lower bound i. Since $P \ge 0$ and $qEN/(mE+nN) \ge 0$, we have

$$\frac{dN}{dt} = rN\left(1-\frac{N}{K}\right) - aN^\alpha P - \frac{qEN}{mE+nN} \le rN\left(1-\frac{N}{K}\right).$$

Because $K(t) \le j$, we have $N/K \ge N/j$ for $N \ge 0$, so $1 - N/K \le 1 - N/j$, and multiplying by $N \ge 0$ preserves the inequality to

give

$$\frac{dN}{dt} \le rN\left(1-\frac{N}{j}\right).$$

By the comparison theorem, $N(t)$ is bounded above by the solution of $\dot{\widetilde{N}} = r\widetilde{N}(1-\widetilde{N}/j)$ with $\widetilde{N}(0) = N(0)$, and this bound satisfies $\widetilde{N}(t) \le \max\{N(0), j\} =: M_N$ throughout the interval of existence. Hence $0 \le N(t) \le M_N$.

Let $W(t) = eN(t) + P(t)$. Differentiating and substituting the system equations gives

$$\begin{aligned}\frac{dW}{dt} &= e\frac{dN}{dt} + \frac{dP}{dt}\\ &= e\left[rN\left(1-\frac{N}{K}\right) - aN^{\alpha}P - \frac{qEN}{mE+nN}\right] + [-d_1P + aeN^{\alpha}P]\\ &= erN\left(1-\frac{N}{K}\right) - \frac{eqEN}{mE+nN} - d_1P.\end{aligned}$$

The predation terms $-aeN^{\alpha}P$ and $+aeN^{\alpha}P$ cancel exactly. Since $eqEN/(mE+nN) \ge 0$, and since Lemma 1 gives $N(1-N/K) \le j/4$, we obtain

$$\frac{dW}{dt} \le \frac{erj}{4} - d_1P.$$

Writing $P = W - eN$ and using the bound $N(t) \le M_N$ established above gives

$$\frac{dW}{dt} \le \frac{erj}{4} - d_1(W-eN) = \frac{erj}{4} + d_1eN - d_1W \le \frac{erj}{4} + d_1eM_N - d_1W.$$

Let $\eta = erj/4 + d_1eM_N$, a positive constant. Then W satisfies the differential inequality

$$\frac{dW}{dt} + d_1W \le \eta.$$

Multiplying by e^{d_1t} and integrating from 0 to t gives

$$W(t) \le W(0)e^{-d_1t} + \frac{\eta}{d_1}\left(1-e^{-d_1t}\right) \le \max\left\{W(0),\ \frac{\eta}{d_1}\right\} =: M_W.$$

Since $W = eN + P$ with $e > 0$ and $N, P \ge 0$, we obtain

$$0 \le N(t) \le \frac{M_W}{e}, \qquad 0 \le P(t) \le M_W.$$

Together with $i \le K(t) \le j$ from Theorem 3.1, every component of the solution of system (2) is bounded on its interval of existence. □

3.1. Equilibrium points

Let $\kappa \in \{i, j\}$ and

$$\begin{aligned}h_\kappa(N) &= r\left(1-\frac{N}{\kappa}\right)(mE+nN) - qE\\ &= -\frac{rn}{\kappa}N^2 + \frac{r}{\kappa}(n\kappa - mE)N + E(rm-q),\end{aligned}$$

$$q_{\mathrm{sn}}(\kappa) = \frac{r(n\kappa+mE)^2}{4nE\kappa} \ge rm, \qquad N_\kappa'^{\pm} = \frac{(n\kappa-mE) \pm \sqrt{\Delta_\kappa}}{2n},$$

$$\Delta_\kappa = (n\kappa-mE)^2 + \frac{4n\kappa E}{r}(rm-q) = \frac{4n\kappa E}{r}\left(q_{\mathrm{sn}}(\kappa)-q\right).$$

Theorem 3.3. *The equilibria of system (2) are the following.*

1. *The extinction equilibrium $E_0 = (0, 0, \kappa)$.*
2. *The predator-free equilibria $(N', 0, \kappa)$, where $N' > 0$ is a root of*
$$h_\kappa(N') = 0. \tag{4}$$
Every positive root of h_κ lies in $(0, \kappa)$, and the equilibria are as follows.
   (a) *If $q < rm$, or if $n\kappa > mE$ and $q = rm$, there is exactly one equilibrium,*
   $$E^s_{1,\kappa} = \left(N_\kappa'^{+},\ 0,\ \kappa\right).$$
   (b) *If $n\kappa > mE$ and $rm < q < q_{\mathrm{sn}}(\kappa)$, there are exactly two equilibria,*
   $$E^-_{1,\kappa} = \left(N_\kappa'^{-},\ 0,\ \kappa\right), \quad E^+_{1,\kappa} = \left(N_\kappa'^{+},\ 0,\ \kappa\right),$$
   where $0 < N_\kappa'^{-} < N_\kappa'^{+} < \kappa$.
   (c) *If $n\kappa > mE$ and $q = q_{\mathrm{sn}}(\kappa)$, the two equilibria of (b) merge into exactly one,*
   $$E^d_{1,\kappa} = \left(\frac{n\kappa-mE}{2n},\ 0,\ \kappa\right).$$
   In all other cases, that is for $q > q_{\mathrm{sn}}(\kappa)$, or for $q \ge rm$ with $n\kappa \le mE$, there is no predator-free equilibrium. The equilibria $E^s_{1,\kappa}$ and $E^+_{1,\kappa}$ are the same branch, given by the larger root $N_\kappa'^{+}$, at different values of q.
3. *The coexistence equilibrium $E_{2,\kappa} = (N^*, P^*_\kappa, \kappa)$, where*
$$N^* = \left(\frac{d_1}{ae}\right)^{1/\alpha} \tag{5}$$
and
$$P^*_\kappa = \frac{1}{a\,(N^*)^{\alpha}}\left[rN^*\left(1-\frac{N^*}{\kappa}\right) - \frac{qEN^*}{mE+nN^*}\right], \tag{6}$$
provided $P^*_\kappa > 0$.

Proof. The right hand side of the third equation of (2) depends only on K, and $l + K > 0$ on the relevant domain, so $dK/dt = 0$ if and only if $\frac{\rho(K-i)}{l+K}\left(1-\frac{K-i}{j-i}\right) = 0$, which holds exactly when $K = i$ or $K = j$. Every equilibrium therefore has the form (N, P, κ) with $\kappa \in \{i, j\}$, where

$$f(N,P) = rN\left(1-\frac{N}{\kappa}\right) - aN^{\alpha}P - \frac{qEN}{mE+nN} = 0,$$
$$g(N,P) = P\left(aeN^{\alpha} - d_1\right) = 0.$$

From $g = 0$ we get $P = 0$ or $N = N^*$. The solution $N = P = 0$ is the extinction equilibrium E_0.

Let $P = 0$ and $N \ne 0$. Then $f = 0$ reads $N\big[r(1-N/\kappa) - qE/(mE+nN)\big] = 0$, and clearing the denominator $mE + nN > 0$ gives $h_\kappa(N) = 0$. This is a concave quadratic whose roots have sum and product

$$S = \frac{n\kappa - mE}{n}, \qquad \Pi = \frac{\kappa E\,(q-rm)}{rn},$$

and whose discriminant is $D = \frac{r^2}{\kappa^2}\Delta_\kappa = \frac{4rnE}{\kappa}\left(q_{\mathrm{sn}}(\kappa) - q\right)$. The identity $(n\kappa+mE)^2 - (n\kappa-mE)^2 = 4n\kappa mE$ gives $q_{\mathrm{sn}}(\kappa) - rm = r(n\kappa-mE)^2/(4nE\kappa) \ge 0$, so $q_{\mathrm{sn}}(\kappa) \ge rm$, with equality if and only if $n\kappa = mE$. Since $h_\kappa(\kappa) = -qE < 0$ and $h_\kappa'(\kappa) = -r(n\kappa + mE)/\kappa < 0$, the concave function h_κ is negative and decreasing on $[\kappa, \infty)$. Hence κ lies to the right of every real root, every positive root lies in $(0, \kappa)$, and only positivity remains to be checked.

For item (a), first let $q < rm$. Then $\Pi < 0$, and $D > 0$ because $q < rm \le q_{\mathrm{sn}}(\kappa)$, so the roots are real with opposite signs. Exactly one of them is positive, namely the larger root $N_\kappa'^{+}$,

and no condition on $n\kappa$ is needed. Next let $n\kappa > mE$ and $q = rm$. Then $\Pi = 0$, so the roots of h_κ are 0 and $S = \kappa - mE/n > 0$. Also $\Delta_\kappa = (n\kappa - mE)^2$, so $N'^{-}_\kappa = 0$ and $N'^{+}_\kappa = (n\kappa - mE)/n = S$. The root 0 is the extinction equilibrium E_0 and is not counted. In both sub-cases exactly one predator-free equilibrium remains, namely $E^s_{1,\kappa} = (N'^{+}_\kappa, 0, \kappa)$.

For item (b), let $n\kappa > mE$ and $rm < q < q_{\mathrm{sn}}(\kappa)$. Then $D > 0$, so the roots are real and distinct and are given by $N'^{\pm}_\kappa$. Since $q > rm$ we have $\Pi > 0$, so the roots are non-zero and share the sign of their sum $S > 0$. Both roots are therefore positive, and the vertex $S/2$ lies strictly between them. Together with $N'^{+}_\kappa < \kappa$ this gives $0 < N'^{-}_\kappa < N'^{+}_\kappa < \kappa$ and the two equilibria $E^-_{1,\kappa}$ and $E^+_{1,\kappa}$. For item (c), let $n\kappa > mE$ and $q = q_{\mathrm{sn}}(\kappa)$. Then $D = 0$, so the two roots of item (b) coincide at the vertex $S/2 = (n\kappa - mE)/(2n)$, which is positive because $n\kappa > mE$. This gives exactly one equilibrium, $E^d_{1,\kappa}$.

In the remaining cases there is no predator-free equilibrium. For $q > q_{\mathrm{sn}}(\kappa)$ we have $D < 0$ and there are no real roots. For $q \geq rm$ with $n\kappa \leq mE$ we have $S \leq 0$. If $q > rm$, the real roots are non-zero with the sign of S, and if $q = rm$ they are 0 and S, so in both cases none is positive. When $n\kappa = mE$ we have $q_{\mathrm{sn}}(\kappa) = rm$, so the whole range $q \geq rm$ gives no positive root. The argument depends on κ only through its value, so it holds at $\kappa = i$ and $\kappa = j$ independently.

Finally, if $N = N^*$, then $f = 0$ is linear in P, with $a(N^*)^\alpha P = rN^*(1 - N^*/\kappa) - qEN^*/(mE + nN^*)$ and the unique solution P^*_κ given in (6). This gives $E_{2,\kappa}$ whenever $P^*_\kappa > 0$, and the condition is evaluated separately at each κ. Since $N^* > 0$, it is a positive root of h_κ, so $E_{2,\kappa}$ coincides with one of the predator-free equilibria in item 2. □

3.2. Feasibility of equilibrium points

Theorem 3.4. *Let $\kappa \in \{i, j\}$. A predator-free equilibrium $(N', 0, \kappa)$ with $N' > 0$ exists if and only if*

$$q < rm \quad \text{or} \quad \Big(n\kappa > mE \ \text{and} \ q \leq q_{\mathrm{sn}}(\kappa)\Big), \tag{7}$$

where $q_{\mathrm{sn}}(\kappa) = r(n\kappa + mE)^2/(4nE\kappa) \geq rm$. When (7) holds, the equilibria are as follows. There are exactly two, $E^-_{1,\kappa}$ and $E^+_{1,\kappa}$, if $n\kappa > mE$ and $rm < q < q_{\mathrm{sn}}(\kappa)$. There is exactly one otherwise, namely $E^s_{1,\kappa}$ if $q < rm$ or if $n\kappa > mE$ and $q = rm$, and $E^d_{1,\kappa}$ if $n\kappa > mE$ and $q = q_{\mathrm{sn}}(\kappa)$.

Proof. The proof follows from Theorem 3.3. □

Theorem 3.5. *The coexistence equilibrium $E_{2,\kappa} = (N^*, P^*_\kappa, \kappa)$ exists at capacity level κ if and only if*

$$q \leq \frac{r}{E}\left(1 - \frac{N^*}{\kappa}\right)(mE + nN^*).$$

Proof. We have from equation (6)

$$P^*_\kappa = \frac{1}{a\,(N^*)^\alpha}\left[rN^*\left(1 - \frac{N^*}{\kappa}\right) - \frac{qEN^*}{mE + nN^*}\right],$$

and since $a(N^*)^\alpha > 0$, the sign of P^*_κ agrees with the sign of the bracketed term. As $N^* > 0$, dividing the bracket by N^* and clearing the denominator $mE + nN^* > 0$ shows

$$rN^*\left(1 - \frac{N^*}{\kappa}\right) - \frac{qEN^*}{mE + nN^*} \ \geq \ 0$$

holds if and only if

$$r\left(1 - \frac{N^*}{\kappa}\right)(mE + nN^*) \ \geq \ qE.$$

Hence $P^*_\kappa > 0$, and $E_{2,\kappa}$ exists, exactly under this condition. Since N^* does not depend on κ, this condition can be evaluated separately at $\kappa = i$ and $\kappa = j$, and $E_{2,i}$ and $E_{2,j}$ can exist simultaneously. □

3.3. Stability of equilibrium points

The Jacobian matrix of system (2) is

$$J(N, P, K) = \begin{pmatrix} F_1 & -aN^\alpha & \dfrac{rN^2}{K^2} \\ ae\alpha N^{\alpha-1}P & aeN^\alpha - d_1 & 0 \\ 0 & 0 & \Gamma(K) \end{pmatrix},$$

where $F_1 = r\left(1 - \dfrac{2N}{K}\right) - a\alpha N^{\alpha-1}P - \dfrac{qEmE}{(mE + nN)^2}$, and $\Gamma(K) = \dfrac{\rho}{j-i}\left[\dfrac{i+j-2K}{l+K} - \dfrac{(K-i)(j-K)}{(l+K)^2}\right]$.

Since the third row has only a diagonal entry, J is block upper triangular, and at any equilibrium (N, P, κ), $\kappa \in \{i, j\}$, its eigenvalues are $\Gamma(\kappa)$ together with those of

$$J_{(N,P)}(N, P, \kappa) = \begin{pmatrix} F_\kappa & -aN^\alpha \\ ae\alpha N^{\alpha-1}P & aeN^\alpha - d_1 \end{pmatrix},$$

where $F_\kappa = r\left(1 - \dfrac{2N}{\kappa}\right) - a\alpha N^{\alpha-1}P - \dfrac{qEmE}{(mE + nN)^2}$.

Evaluating $\Gamma(K)$ at the two roots, the mixed term $(K - i)(j - K)$ vanishes at both $K = i$ and $K = j$, leaving

$$\Gamma(i) = \frac{\rho}{j-i} \cdot \frac{i + j - 2i}{l + i} = \frac{\rho}{l + i} > 0,$$

and

$$\Gamma(j) = \frac{\rho}{j-i} \cdot \frac{i + j - 2j}{l + j} = -\frac{\rho}{l + j} < 0.$$

So the carrying capacity direction is unstable at $\kappa = i$ and stable at $\kappa = j$, and asymptotic stability of $E_{1,\kappa}$ and $E_{2,\kappa}$ is only possible at $\kappa = j$. Consequently, even when $E_{1,i}$ and $E_{2,i}$ exist as equilibria of system (2), they are always unstable, and only $E_{1,j}$ and $E_{2,j}$ can be locally asymptotically stable.

Theorem 3.6. *Let a predator-free equilibrium $(N', 0, j)$ exist, as in Theorem 3.3. Its eigenvalues are $\Gamma(j) < 0$,*

$$\lambda_1 = \frac{N'\,h'_j(N')}{mE + nN'} = N'\left[\frac{qEn}{(mE + nN')^2} - \frac{r}{j}\right], \qquad \lambda_2 = aeN'^{\alpha} - d_1.$$

Then the following hold.

- *(a) For $E^s_{1,j} = (N'^{+}_j, 0, j)$ and for $E^+_{1,j} = (N'^{+}_j, 0, j)$, we have $\lambda_1 < 0$. Hence each is locally asymptotically stable if $aeN'^{+\alpha}_j < d_1$ and is a saddle if $aeN'^{+\alpha}_j > d_1$.*
- *(b) For $E^-_{1,j} = (N'^{-}_j, 0, j)$, we have $\lambda_1 > 0$. Hence $E^-_{1,j}$ is always unstable.*
- *(c) For $E^d_{1,j} = (N_{\mathrm{sn}}, 0, j)$, we have $\lambda_1 = 0$, so $E^d_{1,j}$ is non-hyperbolic. If $d_1 \neq aeN^\alpha_{\mathrm{sn}}$, it is a saddle-node and is unstable. On its center manifold it attracts solutions with $N > N_{\mathrm{sn}}$ and repels those with $N < N_{\mathrm{sn}}$.*

Proof. At $(N', 0, j)$ we have $P = 0$, so $J_{(N,P)}$ is upper triangular,

$$J_{(N,P)}(N', 0, j) = \begin{pmatrix} r\left(1 - \dfrac{2N'}{j}\right) - \dfrac{qEmE}{(mE + nN')^2} & -aN'^{\alpha} \\ 0 & aeN'^{\alpha} - d_1 \end{pmatrix},$$

and its eigenvalues are the diagonal entries λ_1 and λ_2. The third eigenvalue of J is $\Gamma(j) = -\rho/(l + j) < 0$. Since N' is a root of h_j, we have $r(1 - N'/j) = qE/(mE + nN')$, so

$$\begin{aligned} \lambda_1 &= \frac{qE}{mE + nN'} - \frac{rN'}{j} - \frac{qEmE}{(mE + nN')^2} \\ &= N'\left[\frac{qEn}{(mE + nN')^2} - \frac{r}{j}\right]. \end{aligned}$$

Direct differentiation gives $h_j'(N') = -\frac{r}{j}(mE + nN') + \frac{nqE}{mE+nN'}$, and therefore $\lambda_1 = N'h_j'(N')/(mE + nN')$. Because $N' > 0$ and $mE + nN' > 0$, the sign of λ_1 equals the sign of $h_j'(N')$. The function h_j is a concave quadratic with leading coefficient $-rn/j$, so $h_j(N) = -\frac{rn}{j}(N - N_j'^{-})(N - N_j'^{+})$, where $N_j'^{-}$ and $N_j'^{+}$ are the two roots of h_j as in Theorem 3.3.

For item (a), the equilibria $E_{1,j}^s$ and $E_{1,j}^+$ both sit at the larger root $N_j'^{+}$. Differentiating there gives $h_j'(N_j'^{+}) = -\frac{rn}{j}(N_j'^{+} - N_j'^{-}) < 0$, since the roots are distinct. This holds for $q < rm$, where $N_j'^{-} < 0$ and $E_{1,j}^s$ is the only equilibrium, for $q = rm$ with $nj > mE$, where $N_j'^{-} = 0$ and again $E_{1,j}^s$ is the only equilibrium, and for $rm < q < q_{\mathrm{sn}}(j)$ with $nj > mE$, where $N_j'^{-} > 0$ and the equilibrium is $E_{1,j}^+$. Hence $\lambda_1 < 0$, and since $\Gamma(j) < 0$ as well, the sign of λ_2 decides between asymptotic stability, when $\lambda_2 < 0$, and a saddle, when $\lambda_2 > 0$. For item (b), differentiating at the smaller root gives $h_j'(N_j'^{-}) = -\frac{rn}{j}(N_j'^{-} - N_j'^{+}) > 0$, so $\lambda_1 > 0$ and $E_{1,j}^-$ is unstable.

For item (c), the two roots coincide at $N_{\mathrm{sn}} = (nj - mE)/(2n)$, so $h_j'(N_{\mathrm{sn}}) = 0$ and $\lambda_1 = 0$. The other eigenvalues are $\lambda_2 = aeN_{\mathrm{sn}}^{\alpha} - d_1$, which is nonzero by assumption, and $\Gamma(j) < 0$, so the zero eigenvalue is simple and the center eigenvector is $v = (1, 0, 0)^T$. The line $\{P = 0,\ K = j\}$ is invariant, since $P = 0$ is invariant for the P-equation and $K = j$ is an equilibrium of the decoupled K-equation. This line is one-dimensional and tangent to v, so it is a center manifold, and no approximation is needed. The flow on it is

$$\begin{aligned} \dot{N} = f_1(N, 0, j) &= \frac{N\, h_j(N)}{mE + nN} \\ &= -\frac{rn}{j}\,\frac{N\,(N - N_{\mathrm{sn}})^2}{mE + nN}, \end{aligned}$$

because $h_j(N) = -\frac{rn}{j}(N - N_{\mathrm{sn}})^2$ at the double root. For $N > 0$ this is non-positive and vanishes only at $N = N_{\mathrm{sn}}$. Hence N decreases on both sides of N_{sn}, so solutions on the center manifold starting above N_{sn} converge to it, while those starting below it move away toward 0. The reduced equation has a nonzero quadratic term, with coefficient $\frac{1}{2}\partial_N^2 f_1 = -\frac{rnN_{\mathrm{sn}}}{j(mE+nN_{\mathrm{sn}})} \neq 0$, which is the saddle-node structure. By the center manifold theorem, the full system inherits this behavior along the center direction, so the equilibrium is not Lyapunov stable. If $\lambda_2 < 0$, the transverse directions are attracting and $E_{1,j}^d$ is a saddle-node, attracting from $N > N_{\mathrm{sn}}$ and repelling from $N < N_{\mathrm{sn}}$. If $\lambda_2 > 0$, there is in addition an unstable direction in P. In both cases $E_{1,j}^d$ is unstable, which gives (c). □

Theorem 3.7. *Assume $E_{2,j} = (N^*, P_j^*, j)$ exists with $P_j^* > 0$. By definition $N^* = (d_1/ae)^{1/\alpha}$, so $ae(N^*)^{\alpha} = d_1$ and the $(2,2)$ entry of $J_{(N,P)}(E_{2,j})$, namely $ae(N^*)^{\alpha} - d_1$, vanishes identically. Consequently*

$$\operatorname{tr} J_{(N,P)}(E_{2,j}) = A, \qquad \det J_{(N,P)}(E_{2,j}) = a(N^*)^{\alpha}B > 0,$$

where

$$\begin{aligned} A &= r\left(1 - \frac{2N^*}{j}\right) - a\alpha(N^*)^{\alpha-1}P_j^* - \frac{qEmE}{(mE + nN^*)^2}, \\ B &= ae\alpha(N^*)^{\alpha-1}P_j^*. \end{aligned}$$

Hence $E_{2,j}$ is locally asymptotically stable if $A < 0$ and unstable if $A > 0$.

Proof. Since $aeN^{*\alpha} = d_1$, the $(2,2)$ entry of the Jacobian vanishes, so

$$J_{(N,P)}(E_{2,j}) = \begin{pmatrix} A & -a(N^*)^{\alpha} \\ B & 0 \end{pmatrix}.$$

Thus $\mathrm{tr} = A$ and $\det = a(N^*)^{\alpha}B > 0$ because $P_j^* > 0$. For a 2×2 matrix with positive determinant, both eigenvalues have negative real part iff $\mathrm{tr} < 0$, and positive real part iff $\mathrm{tr} > 0$. The third eigenvalue is $\Gamma(j) = -\rho/(l + j) < 0$. Hence $E_{2,j}$ is locally asymptotically stable if $A < 0$ and unstable if $A > 0$. □

3.4. Bifurcation analysis

Theorem 3.8. *Let $(N', 0, j)$ be one of $E_{1,j}^s$, $E_{1,j}^+$ or $E_{1,j}^-$, with $q \neq q_{\mathrm{sn}}(j)$. Then system (2) undergoes a transcritical bifurcation at $(N', 0, j)$ when d_1 passes through $d_{1,\mathrm{TC}} = ae\,(N')^{\alpha}$, at which $E_{2,j}$ coincides with $(N', 0, j)$.*

Proof. The point $(N', 0, j)$ does not depend on d_1, so it is an equilibrium for every d_1. At $d_1 = d_{1,\mathrm{TC}}$ we have $N^* = (d_1/(ae))^{1/\alpha} = N'$, hence $P_j^* = 0$ and $E_{2,j}$ coincides with $(N', 0, j)$. The eigenvalues of J are λ_1, λ_2 and $\Gamma(j)$. Here $\lambda_2 = ae(N')^{\alpha} - d_1 = 0$, while $\Gamma(j) = -\rho/(l + j) < 0$ and, by Theorem 3.6, $\lambda_1 \neq 0$ because $q \neq q_{\mathrm{sn}}(j)$. So $\lambda_2 = 0$ is a simple eigenvalue and the other two have nonzero real part, and we apply Sotomayor's theorem [15] with d_1 as the bifurcation parameter.

At the bifurcation point the Jacobian is

$$J = \begin{pmatrix} \lambda_1 & -a_0 & c \\ 0 & 0 & 0 \\ 0 & 0 & \Gamma(j) \end{pmatrix}.$$

Solving $Jv = 0$, the third row gives $\Gamma(j)v_3 = 0$, so $v_3 = 0$, and the first row gives $\lambda_1 v_1 - a_0 v_2 = 0$. Taking $v_2 = \lambda_1$ gives $v = (a_0, \lambda_1, 0)^T$. Solving $w^T J = 0$, the first column gives $\lambda_1 w_1 = 0$, so $w_1 = 0$, and the third column gives $cw_1 + \Gamma(j)w_3 = 0$, so $w_3 = 0$. Taking $w_2 = 1$ gives $w = (0, 1, 0)^T$.

Writing system (2) as $\dot{X} = f(X, d_1)$ with $X = (N, P, K)^T$, only f_2 depends on d_1, and $f_{d_1} = (0, -P, 0)^T$. This vanishes at $P = 0$, so $f_{d_1}(X_0, d_{1,\mathrm{TC}}) = 0$ and the first condition holds,

$$w^T f_{d_1}(X_0, d_{1,\mathrm{TC}}) = 0.$$

The derivative of f_{d_1} with respect to X has a single nonzero entry, $\partial_P(-P) = -1$ in position $(2,2)$, so $Df_{d_1}v = (0, -v_2, 0)^T$ and the

second condition holds,

$$w^T\big[Df_{d_1}(X_0, d_{1,\mathrm{TC}})v\big] = -v_2 = -\lambda_1 \neq 0.$$

For the third condition, only f_2 contributes because $w = (0,1,0)^T$. Since $f_2 = P(aeN^\alpha - d_1)$,

$$\begin{aligned}\frac{\partial^2 f_2}{\partial N \partial P} &= ae\alpha N^{\alpha-1},\\ \frac{\partial^2 f_2}{\partial N^2} &= ae\alpha(\alpha-1)N^{\alpha-2}P = 0,\\ \frac{\partial^2 f_2}{\partial P^2} &= 0\end{aligned}$$

at $P = 0$. So, with $v = (a_0, \lambda_1, 0)^T$ this gives

$$\begin{aligned}w^T\big[D^2 f(X_0, d_{1,\mathrm{TC}})(v,v)\big] &= 2v_1 v_2\, ae\alpha(N')^{\alpha-1}\\ &= 2a_0\lambda_1\, ae\alpha(N')^{\alpha-1}\\ &\neq 0.\end{aligned}$$

All three conditions of Sotomayor's theorem hold, so a transcritical bifurcation occurs. When h_j has two positive roots, the argument applies to $E^-_{1,j}$ and $E^+_{1,j}$ separately, which gives the two values $d^{\pm}_{1,\mathrm{TC}} = ae\,(N'^{\pm}_j)^\alpha$. □

Theorem 3.9. *Fix d_1 so that $N^* = (d_1/(ae))^{1/\alpha} \in (0, j)$, assume $N^* \neq N_{\mathrm{sn}}$, and put*

$$q_{\mathrm{thresh}} = \frac{r}{E}\Big(1 - \frac{N^*}{j}\Big)(mE + nN^*).$$

Then system (2) undergoes a transcritical bifurcation when q passes through q_{thresh}, at which $E_{2,j}$ coincides with the predator-free equilibrium $(N^*, 0, j)$. This equilibrium is $E^-_{1,j}$ if $N^* < N_{\mathrm{sn}}$ and $E^+_{1,j}$ or $E^s_{1,j}$ if $N^* > N_{\mathrm{sn}}$.

Proof. At $q = q_{\mathrm{thresh}}$ we have $h_j(N^*) = 0$, so N^* is a positive root of h_j, and $P^*_j = 0$, so $E_{2,j}$ coincides with $(N^*, 0, j)$. Since $h'_j(N) = -\frac{2rn}{j}(N - N_{\mathrm{sn}})$, we have $h'_j(N^*) \neq 0$ exactly when $N^* \neq N_{\mathrm{sn}}$. If $h'_j(N^*) > 0$ then N^* is the smaller root and the equilibrium is $E^-_{1,j}$, and if $h'_j(N^*) < 0$ it is the larger root. Hence $\lambda_1 = N^* h'_j(N^*)/(mE + nN^*) \neq 0$, while $\lambda_2 = ae(N^*)^\alpha - d_1 = 0$ and $\Gamma(j) < 0$, so the zero eigenvalue is simple.

We cannot apply Sotomayor's conditions to f directly. Only f_1 depends on q, and $w = (0,1,0)^T$ annihilates it, so the second condition would give 0 even though the branches do cross. The predator-free branch moves with q while $E_{2,j}$ stays on $N = N^*$, so we follow the branch. Since $h'_j(N^*) \neq 0$ and $\partial_q h_j = -E$, the implicit function theorem gives a smooth root $N'(q)$ of $h_j(\cdot\,; q)$ near q_{thresh} with $N'(q_{\mathrm{thresh}}) = N^*$ and

$$N'_q = \frac{E}{h'_j(N')}.$$

Put $x = N - N'(q)$. Because q is a constant parameter, the shift adds no extra term, and the system in the variables (x, P, K) is $\dot X = F(X, q)$ with

$$F = \big(f_1(N' + x, P, K, q),\ P\,(ae(N' + x)^\alpha - d_1),\ H(K)\big)^T.$$

Now $F(0, 0, j; q) = 0$ for all q near q_{thresh}, so the predator-free equilibrium sits at the origin throughout. At $q = q_{\mathrm{thresh}}$ the Jacobian at the origin equals J above with $N' = N^*$, so $v = (a_0, \lambda_1, 0)^T$ and $w = (0,1,0)^T$ with $a_0 = a(N^*)^\alpha$.

The first component of F_q is

$$\partial_N f_1\, N'_q + \partial_q f_1 = \frac{d}{dq} f_1(N'(q), 0, j, q) = 0$$

at $P = 0$, $x = 0$, because $f_1(N'(q), 0, j, q) \equiv 0$. The second component is

$$F_{2,q} = ae\alpha(N' + x)^{\alpha-1} N'_q\, P,$$

which vanishes at $P = 0$. Hence $F_q = 0$ at the bifurcation point and the first condition holds, $w^T F_q = 0$. For the second condition, only $F_{2,q}$ contributes, and its only nonzero derivative at the origin is $\partial_P F_{2,q} = ae\alpha(N^*)^{\alpha-1} N'_q$. Using $\lambda_1 = N^* h'_j(N^*)/(mE + nN^*)$, $N'_q = E/h'_j(N^*)$ and $ae(N^*)^\alpha = d_1$,

$$\begin{aligned}w^T\big[DF_q\, v\big] &= \lambda_1\, ae\alpha(N^*)^{\alpha-1} N'_q\\ &= \frac{N^* h'_j(N^*)}{mE + nN^*}\, ae\alpha(N^*)^{\alpha-1}\frac{E}{h'_j(N^*)}\\ &= \frac{\alpha d_1 E}{mE + nN^*}\\ &\neq 0.\end{aligned}$$

For the third condition, only $\partial^2 F_2/\partial x \partial P = ae\alpha(N^*)^{\alpha-1}$ survives at $P = 0$, exactly as in Theorem 3.8, so

$$w^T\big[D^2 F(v,v)\big] = 2a_0\lambda_1\, ae\alpha(N^*)^{\alpha-1} \neq 0.$$

Sotomayor's conditions hold for F, and since the shift is a smooth change of coordinates depending smoothly on q, the bifurcation diagram of f is the same. A transcritical bifurcation occurs, with $E_{2,j}$ existing for $q \le q_{\mathrm{thresh}}$ by Theorem 3.5. □

Theorem 3.10. *Assume $nj > mE$ and $d_1 \neq ae\,N^\alpha_{\mathrm{sn}}$. Then system (2) undergoes a saddle-node bifurcation at $q = q_{\mathrm{sn}}(j) = r(nj + mE)^2/(4nEj)$. For $rm < q < q_{\mathrm{sn}}(j)$ the equilibria $E^-_{1,j}$ and $E^+_{1,j}$ exist, at $q = q_{\mathrm{sn}}(j)$ they merge into $E^d_{1,j} = (N_{\mathrm{sn}}, 0, j)$, and for $q > q_{\mathrm{sn}}(j)$ no predator-free equilibrium exists.*

Proof. The existence statements follow from Theorem 3.3. At $E^d_{1,j}$ we have $h_j(N_{\mathrm{sn}}) = h'_j(N_{\mathrm{sn}}) = 0$, so $\lambda_1 = 0$, while $\lambda_2 = aeN^\alpha_{\mathrm{sn}} - d_1 \neq 0$ and $\Gamma(j) < 0$. The zero eigenvalue is therefore simple, and the Jacobian is

$$J = \begin{pmatrix} 0 & -a_0 & c\\ 0 & \lambda_2 & 0\\ 0 & 0 & \Gamma(j)\end{pmatrix},$$

where $a_0 = aN^\alpha_{\mathrm{sn}}$, and $c = \frac{rN^2_{\mathrm{sn}}}{j^2}$.

Solving $Jv = 0$, the third row gives $v_3 = 0$ and the second gives $\lambda_2 v_2 = 0$, so $v_2 = 0$. Taking $v_1 = 1$ gives $v = (1, 0, 0)^T$. Solving $w^T J = 0$, the second column gives $-a_0 w_1 + \lambda_2 w_2 = 0$ and the third gives $cw_1 + \Gamma(j)w_3 = 0$. Taking $w_1 = 1$ gives

$$w = \Big(1,\ \frac{a_0}{\lambda_2},\ -\frac{c}{\Gamma(j)}\Big)^T.$$

Writing system (2) as $\dot X = f(X, q)$, only f_1 depends on q, with $f_{1,q} = -EN/(mE + nN)$, so $f_q = (f_{1,q}, 0, 0)^T$. Using $N_{\mathrm{sn}} = (nj - mE)/(2n)$ and $mE + nN_{\mathrm{sn}} = (nj + mE)/2$, the first condition for

a saddle-node holds,

$$\begin{aligned} w^T f_q(X_0, q_{\text{sn}}) &= -\frac{EN_{\text{sn}}}{mE + nN_{\text{sn}}} \\ &= -\frac{E\,(nj - mE)}{n\,(nj + mE)} \\ &\neq 0. \end{aligned}$$

For the second condition, $v = (1, 0, 0)^T$ selects the pure second derivatives in N. Now f_2 carries the factor $P = 0$, and $f_3 = H(K)$ does not depend on N, so only $\partial_N^2 f_1$ contributes and $w^T D^2 f(v, v) = \partial_N^2 f_1$. On $P = 0, K = j$,

$$f_1 = \frac{N\,h_j(N)}{mE + nN}.$$

Differentiating twice and using $h_j = h_j' = 0$ and $h_j'' = -2rn/j$ at N_{sn}, only the term with h_j'' survives,

$$\begin{aligned} w^T\big[D^2 f(X_0, q_{\text{sn}})(v, v)\big] &= \frac{N_{\text{sn}} h_j''}{mE + nN_{\text{sn}}} \\ &= -\frac{2r\,(nj - mE)}{j\,(nj + mE)} \\ &\neq 0. \end{aligned}$$

Both conditions of Sotomayor's theorem for a saddle-node bifurcation hold. □

Theorem 3.11. *The system (2) undergoes a Hopf bifurcation at the interior equilibrium point $E_{2,j} = (N^*, P_j^*, j)$ with respect to a parameter μ at a critical value $\mu = \mu_H$, provided*

$$A(\mu_H) = 0,$$

where

$$A = r\left(1 - \frac{2N^*}{j}\right) - a\alpha (N^*)^{\alpha-1} P_j^* - \frac{qEmE}{(mE + nN^*)^2},$$

and the transversality condition

$$\left.\frac{dA}{d\mu}\right|_{\mu=\mu_H} \neq 0$$

holds.

Proof. By Theorem 3.7, the eigenvalues of $J_{(N,P)}(E_{2,j})$ satisfy $\operatorname{tr} J_{(N,P)}(E_{2,j}) = A$ and $\det J_{(N,P)}(E_{2,j}) = a(N^*)^\alpha B > 0$, with $B = ae\alpha (N^*)^{\alpha-1} P_j^* > 0$, so the characteristic equation of this block is

$$\lambda^2 - A\lambda + \det J_{(N,P)}(E_{2,j}) = 0.$$

Since $\det J_{(N,P)}(E_{2,j}) > 0$ for every admissible parameter value, a Hopf bifurcation occurs precisely when A passes through zero, at which point the roots become purely imaginary, $\lambda_{1,2}(\mu_H) = \pm i\sqrt{\det J_{(N,P)}(E_{2,j})}$, while the third eigenvalue $\Gamma(j) = -\rho/(l + j)$ remains strictly negative throughout, since it does not depend on μ through A.

For transversality, let $\lambda(\mu) = \sigma(\mu) \pm i\omega(\mu)$ denote the complex conjugate pair, with $\sigma(\mu_H) = 0$. Differentiating the characteristic equation with respect to μ gives

$$2\lambda\dot{\lambda} - \dot{A}\lambda - A\dot{\lambda} + \dot{\det} = 0,$$

where the overdot denotes differentiation with respect to μ. At $\mu = \mu_H$, $A = 0$ and $\lambda = i\omega_0$ with $\omega_0 = \sqrt{\det J_{(N,P)}(E_{2,j})}$, so

$$\dot{\lambda}\big|_{\mu_H} = \frac{\dot{A}\, i\omega_0 - \dot{\det}}{2i\omega_0} = \frac{\dot{A}}{2} + i\frac{\dot{\det}}{2\omega_0}.$$

Taking the real part gives

$$\left.\frac{d\sigma}{d\mu}\right|_{\mu_H} = \frac{1}{2}\left.\frac{dA}{d\mu}\right|_{\mu_H}.$$

Hence the transversality condition $d\sigma/d\mu|_{\mu_H} \neq 0$ holds if and only if $dA/d\mu|_{\mu_H} \neq 0$. When this holds, the complex conjugate eigenvalues cross the imaginary axis transversally, and system (2) undergoes a Hopf bifurcation at $E_{2,j}$ as μ passes through μ_H.

The parameters of Table 1, gives $a_1 \approx -1.67 \times 10^{-4} < 0$. Together with $dA/dd_1|_{d_{1,H}} < 0$, this shows that the Hopf bifurcation is supercritical. □

3.5. Explicit solution and recovery dynamics of the variable carrying capacity

Theorem 3.12. *Let $K(t)$ solve equation (1) with $K(0) = K_0 \in (i, j)$. Then, for every finite $t \geq 0$, $K(t)$ is given implicitly by*

$$t = \frac{1}{\rho}\left[(l + i)\ln\frac{K - i}{K_0 - i} - (l + j)\ln\frac{j - K}{j - K_0}\right]. \tag{8}$$

Proof. By Theorem 3.1, $K(t) \in (i, j)$ for every finite $t \geq 0$ whenever $K_0 \in (i, j)$, so

$$\begin{aligned} dt &= \frac{(l + K)(j - i)}{\rho(K - i)(j - K)}dK \\ \implies dt &= \frac{1}{\rho}\left[\frac{l + i}{K - i} + \frac{l + j}{j - K}\right]dK. \end{aligned}$$

Integrating both sides from K_0 to K, and using $K \in (i, j)$ so that $K - i > 0$ and $j - K > 0$ throughout, gives

$$\begin{aligned} t &= \frac{1}{\rho}\Big[(l + i)\ln(K - i) - (l + j)\ln(j - K)\Big]_{K_0}^{K} \\ &= \frac{1}{\rho}\left[(l + i)\ln\frac{K - i}{K_0 - i} - (l + j)\ln\frac{j - K}{j - K_0}\right], \end{aligned}$$

as claimed. □

Corollary 3.12.1. *Let $\eta \in (0, 1)$ and define $K_\eta = i + \eta(j - i)$, where K_η is the carrying-capacity level located at a fraction η of the distance from the lower equilibrium i to the upper equilibrium j. If $K_0 < K_\eta$, then the time T_η required for $K(t)$ to reach K_η is given by*

$$T_\eta = \frac{1}{\rho}\left[(l + i)\ln\frac{\eta(j - i)}{K_0 - i} - (l + j)\ln\frac{(1 - \eta)(j - i)}{j - K_0}\right]. \tag{9}$$

Proof. Substitute $K = K_\eta$ into equation (8), using $K_\eta - i = \eta(j - i)$ and $j - K_\eta = (1 - \eta)(j - i)$. □

The corollary provides an explicit measure of the recovery time of the carrying capacity from an initial level K_0 to any prescribed intermediate level K_η between the lower equilibrium i and the upper equilibrium j. Thus, T_η quantifies how rapidly the carrying capacity recovers toward its maximum sustainable level.

Theorem 3.13. *Let $\rho > 0$ be fixed. Then for every $K \in (i, j)$, the instantaneous recovery rate $H(K)$ is strictly decreasing in l,*

$$\frac{\partial H}{\partial l}(K) < 0.$$

Consequently, for every $\eta \in (0,1)$ with $K_0 < K_\eta$, the recovery time T_η of Corollary 3.12.1 is strictly increasing in l, at fixed ρ,

$$\frac{\partial T_\eta}{\partial l} > 0.$$

Proof. Writing $H(K) = \rho(K-i)(j-K)/[(l+K)(j-i)]$ and differentiating with respect to l,

$$\frac{\partial H}{\partial l}(K) = -\frac{\rho(K-i)(j-K)}{(j-i)(l+K)^2}.$$

For $K \in (i,j)$ we have $K-i>0$ and $j-K>0$, and ρ, $j-i$, $(l+K)^2$ are all strictly positive, so $\partial H/\partial l(K) < 0$.

For the recovery time, differentiate equation (9) directly with respect to l,

$$\frac{\partial T_\eta}{\partial l} = \frac{1}{\rho}\left[\ln\frac{\eta(j-i)}{K_0-i} - \ln\frac{(1-\eta)(j-i)}{j-K_0}\right].$$

Since $K_0 < K_\eta = i+\eta(j-i)$, we have $K_0 - i < \eta(j-i)$, so the argument of the first logarithm exceeds 1. Since $K_0 < K_\eta < j$, we have $j-K_0 > j-K_\eta = (1-\eta)(j-i)$, so the argument of the second logarithm is less than 1. Hence the first term is positive and the subtracted second term is negative, giving $\partial T_\eta/\partial l > 0$. □

4. Numerical analysis

In this section, we present numerical simulations of our given dynamical system to demonstrate the obtained theoretical results. Since real ecological data are unavailable for all parameters introduced in this work we obtain the baseline values given in the Table 1, by performing time-series simulations of proposed system in and selecting a regime in which $N(t), P(t)$ simultaneously exhibit sustained oscillations, so that the dynamics can illustrate the stability and bifurcation results established above. We fix the values of the other parameters to the values outlined in the table below and modify the value of the parameter we are going to study as needed.

Since N^α is not locally Lipschitz at $N=0$, it is evaluated as $\max(N,0)^\alpha$ throughout, guarding against negative or complex values near the boundary. This guard leaves the dynamics unchanged whenever $N(t) > 0$, and for every simulation reported below $N(t)$ remains bounded well away from zero.

4.1. Nullclines of the system

This section illustrates the influence of the catchability coefficient q on the nullclines of the system. The solid curves represent the prey nullcline

$$P = \frac{1}{aN^\alpha}\left[rN\left(1-\frac{N}{j}\right) - \frac{qEN}{mE+nN}\right]$$

while the vertical dashed line is the predator nullcline $N = N^* = (d_1/ae)^{1/\alpha}$. Since the predator nullcline $N = N^*$ is independent of q, harvesting acts solely through the prey nullcline, whose height at $N = N^*$ determines the predator density P_j^* at coexistence. As q increases, the prey nullcline shifts downward, causing the coexistence equilibrium $E_{2,j} = (N^*, P_j^*, j)$ to descend along the fixed vertical line $N = N^*$. At $q = 0.03$, the intersection occurs at $E_{2,j} = (2.9269, 3.4272)$; increasing the catchability coefficient to $q = 0.35$ lowers this to $E_{2,j} = (2.9269, 1.3402)$. At the threshold value $q = q_{\text{thresh}} \approx 0.5555$, given by Theorem 3.5 as

$$q_{\text{thresh}} = \frac{r}{E}\left(1-\frac{N^*}{j}\right)(mE+nN^*),$$

Table 1. Model parameters used in the simulations

Symbol	Value	Unit
r	0.2	time^{-1}
q	0.03	time^{-1}
a	0.06	population$^{-\alpha}$ time^{-1}
E	1.0	dimensionless
α	0.6	dimensionless
m	1.0	dimensionless
d_1	0.08	time^{-1}
n	1.0	population^{-1}
e	0.7	dimensionless
l	5	population
ρ_0	0.1	time^{-1}
ρ	0.5	population $\cdot$ time^{-1}
i	1	population
j	10	population

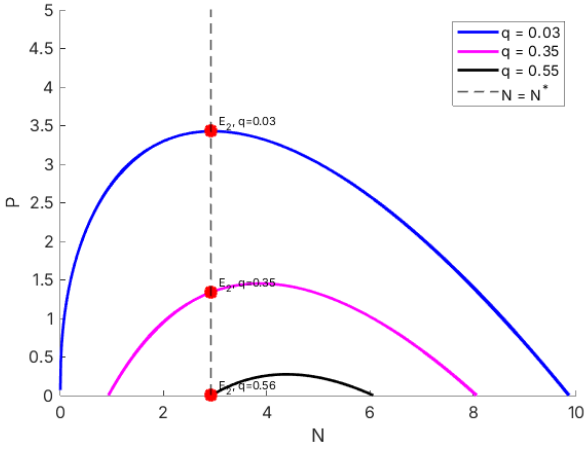


Figure 1. Nullclines of the system (2) in the (N,P) phase plane for three values of the catchability coefficient q. The coexistence equilibrium $E_{2,j}$ is indicated for each value of q.

the prey nullcline intersects the predator nullcline exactly at $P_j^* = 0$, so that $E_{2,j}$ coincides with the boundary equilibrium $E_{1,j}$ on the N-axis. Beyond this threshold, $q > q_{\text{thresh}}$, the prey nullcline no longer reaches $N = N^*$ at a positive height. Consequently, the two nullclines do not intersect in the open first quadrant, and the coexistence equilibrium ceases to exist. This progression demonstrates that harvesting not only reduces the predator density at coexistence but, beyond a critical effort level, eliminates the coexistence equilibrium entirely, leaving only the predator-free state $E_{1,j}$ as the biologically relevant equilibrium.

4.2. Time series and comparison with the constant carrying capacity model

Figure 2 compares the variable carrying capacity model (2), in which $K(t)$ evolves according to equation (1), with the constant carrying capacity model obtained by fixing $K \equiv j$ and keeping all other parameters identical. In panel (c), $K(t)$ rises monotonically to $j = 10$ and remains there. This is consistent with $\Gamma(j) = -\rho/(l+j) < 0$, and since $dK/dt > 0$ on (i,j), every solution with $K(0) \in (i,j)$ converges monotonically to j. Once $K(t) \approx j$, the variable-K system reduces to the constant-K system.

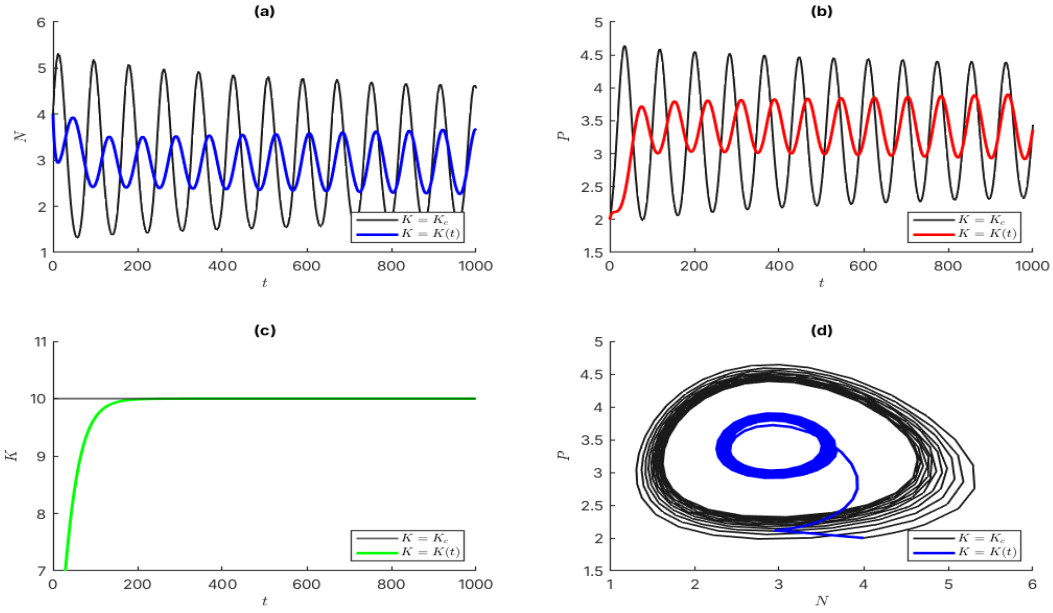


Figure 2. Time series comparison between the variable carrying capacity model (2) (shown in colored lines) and the corresponding constant carrying capacity model for identical predator–prey parameters (in black lines).

Both models show sustained oscillations rather than convergence to $E_{2,j}$, consistent with Theorem 3.11. Here $d_1 = 0.08$ lies just below the Hopf threshold $d_{1,H} \approx 0.0804$, so the trace A is positive and $E_{2,j}$ is unstable. Panel (d) shows both trajectories spiralling outward onto closed orbits in the (N, P) plane.

The models differ only in the transient. While $K(t) < j$, the prey is limited by a smaller carrying capacity, which changes the early oscillations in panels (a) and (b). Since the carrying-capacity equation is autonomous and $K = j$ attracts every solution with $K(0) \in (i, j)$, the limiting (N, P) dynamics are those of the constant-K model, independent of l, i and the history of $K(t)$.

4.3. Sensitivity of the carrying capacity dynamics

In this section we illustrate the behaviour of the carrying-capacity equation (1) in isolation from the full predator–prey dynamics, in Figure 3, showing how the parameters l and i introduced in our generalisation of the Meyer–Ausubel formulation affect environmental recovery from a depleted state.

Panel (a) shows the effect of the saturation constant l. As l increases, the per-capita growth rate $\rho/(l + K)$ decreases throughout the admissible range $[i, j]$, substantially slowing the recovery of $K(t)$ toward j. For $l = 0.5$, $K(t)$ reaches its equilibrium level within roughly $t \approx 100$, whereas for $l = 50$ the trajectory remains close to its minimum value even after $t = 300$. This behaviour is consistent with the asymptotic reduction discussed in the Introduction, where the shifted logistic law is recovered as $l \to \infty$ with rate $\rho_0 = \rho/l$. Since ρ is held fixed in Figure 3(a), increasing l decreases ρ_0, which is why the recovery slows. The results demonstrate that moderate increases in l can substantially lengthen the environmental recovery time-scale, an effect absent from the classical Meyer–Ausubel model and arising from the saturation introduced in the present formulation.

Panel (b) shows the effect of the minimum carrying capacity i, with l held fixed. Although increasing i places the initial condition closer to the equilibrium level j, the trajectories do not recover monotonically faster. In particular, the curve for $i = 5$ exhibits a longer initial plateau than those for $i = 0.5$ and $i = 2$ before accelerating toward j. This behaviour follows from the local growth rate at the lower boundary,

$$\Gamma(i) = \frac{\rho}{l + i},$$

which decreases strictly as i increases. Here, $\Gamma(i) = 0.0909, 0.0714, 0.0500$ for the parameter values $i = 0.5, 2, 5$, respectively. Thus, a larger minimum carrying capacity produces a weaker initial departure rate from $K = i$, which can outweigh the shorter distance $(j - i)$ to the equilibrium. Consequently, the recovery time-scale is influenced by the local dynamics near the lower boundary rather than by proximity to the target carrying capacity alone.

4.4. Effect of the group defence parameter α

We illustrate the effect of the group defence parameter α on the dynamics at $E_{2,j}$ in Figure 4. For $\alpha = 0.3$ panels (a) and (d) show the trajectory spiralling directly toward the interior equilibrium, consistent with a negative trace A and hence local asymptotic stability of $E_{2,j}$ by Theorem 3.7. As α increases to 0.6, panels (b) and (e) show that the trace A becomes positive, rendering the equilibrium unstable and causing the trajectory to approach a stable limit cycle with sustained, near-periodic oscillations characteristic of a Hopf bifurcation. Increasing α further to 0.85, panels (c) and (f) show the trajectory once again spiralling toward a stable interior equilibrium, although at a different population level from that in panel (a).

This non-monotonic pattern, with stability at low and high α and an intervening oscillatory pattern, shows that the group defence exponent does not act as a uniformly stabilising or destabilising parameter over its range $\alpha \in (0, 1]$. Instead, the sign of the trace $A = r(1 - 2N^*/j) - a\alpha(N^*)^{\alpha-1}P_j^* - qEmE/(mE +$

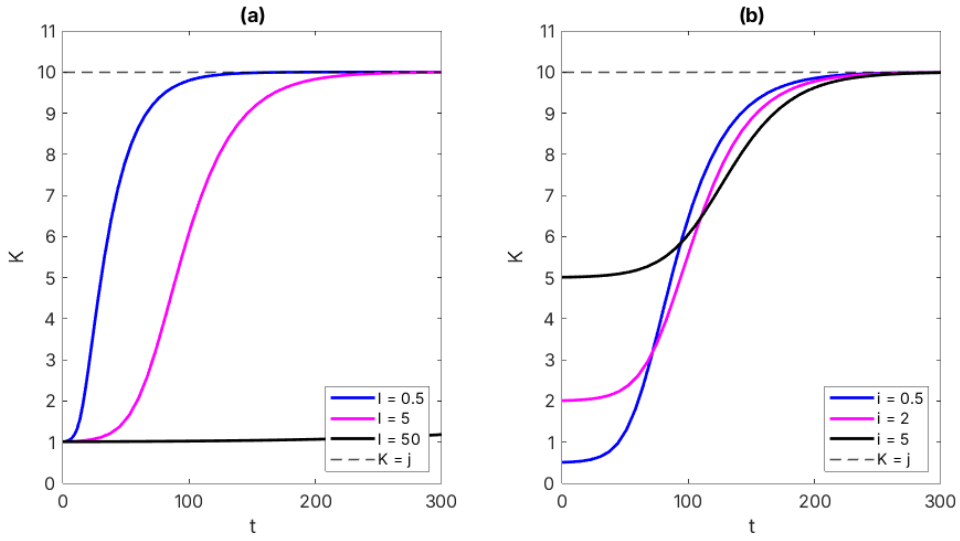


Figure 3. Trajectories of the carrying capacity $K(t)$, obtained by integrating equation (1) in isolation from an initial condition just above its lower bound. Panel (a) varies the saturation constant l with i fixed at its default value; panel (b) varies the minimum carrying capacity i with l fixed at its default value. In both panels, K converges to the equilibrium level $K = j$ (dashed line).

$nN^*)^2$ depends on α through both the explicit dependence of the middle term and the implicit dependence of $N^* = (d_1/ae)^{1/\alpha}$ and P_j^* on α. This allows the system to cross the Hopf boundary twice as α varies over the considered range. Thus, in this parameter space, intermediate levels of group defence can produce oscillatory dynamics between stable regimes at lower and higher values of α, highlighting the ecological significance of the parameter α in the model.

4.5. Effect of the predator mortality rate d_1

We discuss the effect of the predator mortality rate d_1 on the dynamics at $E_{2,j}$ in Figure 5. For $d_1 = 0.078$, panels (a) and (d) show sustained oscillations of relatively large and somewhat irregular amplitude. The trajectory has not yet settled onto a smooth closed orbit within the simulated time window, suggesting that the system is close to, but has not fully reached, its limiting cycle. Increasing d_1 slightly to 0.08, panels (b) and (e) show a cleaner, smaller-amplitude limit cycle, indicating faster convergence and reduced oscillation amplitude within this unstable regime. At $d_1 = 0.15$, panels (c) and (f) show the trajectory spiralling inward toward a stable interior equilibrium, indicating that the coexistence state has regained stability.

Unlike the non-monotonic response to α, the transition with d_1 is monotonic. Increasing predator mortality progressively reduces the oscillation amplitude until the Hopf threshold is crossed and $E_{2,j}$ becomes stable, consistent with Theorem 3.11. Biologically, this indicates that higher predator mortality acts as a stabilising mechanism in this model. This contrasts with catchability coefficient q, which, destabilises the coexistence state by driving the system toward loss of the coexistence equilibrium rather than merely reducing the oscillation amplitude.

4.6. Stability regions of predator-free and coexistence equilibria

We partition the (q, d_1) parameter plane according to the feasibility and local stability of the predator-free equilibria $E_{1,j}$ and of the interior equilibrium $E_{2,j}$, in Figures 6 and 7, with all other parameters fixed at the values in Table 1. The relevant conditions are given by Theorems 3.3, 3.4, 3.6, 3.5 and 3.7. For these parameters $rm = 0.2$ and $q_{\text{sn}}(j) = r(nj + mE)^2/(4nEj) = 0.605$.

In Figure 6, the number of predator-free equilibria depends only on q (Theorem 3.3). For $q < rm$ there is a single equilibrium $E_{1,j}^s$. At $q = rm$ the smaller root $N_j'^-$ crosses zero, so for $rm < q < q_{\text{sn}}(j)$ there are two equilibria, $E_{1,j}^-$ and $E_{1,j}^+$. At $q = q_{\text{sn}}(j)$ they merge into the repeated root $E_{1,j}^d$, a saddle-node that is unstable and for $q > q_{\text{sn}}(j)$ there is no predator-free equilibrium. By Theorem 3.6, $E_{1,j}^-$ is always unstable, and $E_{1,j}^s$, $E_{1,j}^+$ are stable if and only if $d_1 > ae\,(N_j'^+)^\alpha$ and are saddles otherwise. This stability boundary decreases with q, from $d_1 \approx 0.167$ as $q \to 0$ to 0.157 at $q = rm$, 0.143 at $q = 0.4$ and 0.110 at $q = 0.6$, and reaches 0.1036 at $q_{\text{sn}}(j)$. Thus predator-free stability is governed by predator mortality relative to predator growth at $N_j'^+$, with harvesting also lowering the required mortality appreciably once q is large.

Figure 7 shows a different structure. By Theorem 3.5, $E_{2,j}$ exists iff $P_j^* > 0$, that is, iff $N_j'^- < N^* < N_j'^+$ or equivalently $ae\,(N_j'^-)^\alpha < d_1 < ae\,(N_j'^+)^\alpha$, where the lower bound is absent for $q \le rm$. Both bounds are the transcritical curves of Theorems 3.8 and 3.9, at which $E_{2,j}$ meets $E_{1,j}^\mp$. For $q > rm$ the lower bound rises with q (from 0.031 at $q = 0.3$ to 0.097 at $q = 0.6$) while the upper bound falls, so the feasible region narrows into a wedge. It closes at $q = q_{\text{sn}}(j)$, where the two curves meet at $d_1 = ae\,N_{\text{sn}}^\alpha \approx 0.1036$, and not near $q \approx 0.56$. The upper bound is the stability boundary of $E_{1,j}^+$, which is not the condition $N^* < j$ alone, so $E_{2,j}$ and a stable $E_{1,j}^+$ are never simultaneously feasible: where $E_{2,j}$ exists, $E_{1,j}^+$ is a saddle. Within the wedge, $E_{2,j}$ is unstable ($A > 0$) below the Hopf curve $d_1 = d_{1,H}(q)$ and stable ($A < 0$) above it. Numerically, $d_{1,H}$ increases with q: 0.0804 at $q = 0.03$, 0.0884 at $q = 0.2$, 0.0965 at $q = 0.4$ and 0.1034 at $q = 0.6$. Increasing harvesting therefore shifts the coexistence equilibrium from the stable to the unstable regime, consistent with the condition $A < 0$.

4.7. Verification of Transcritical and Saddle-Node bifurcations

We illustrate the two transcritical bifurcations and the saddle-node bifurcation identified analytically in Theorems 3.9, 3.8 and 3.10 in Figure 8. Only the prey density N is shown, since the

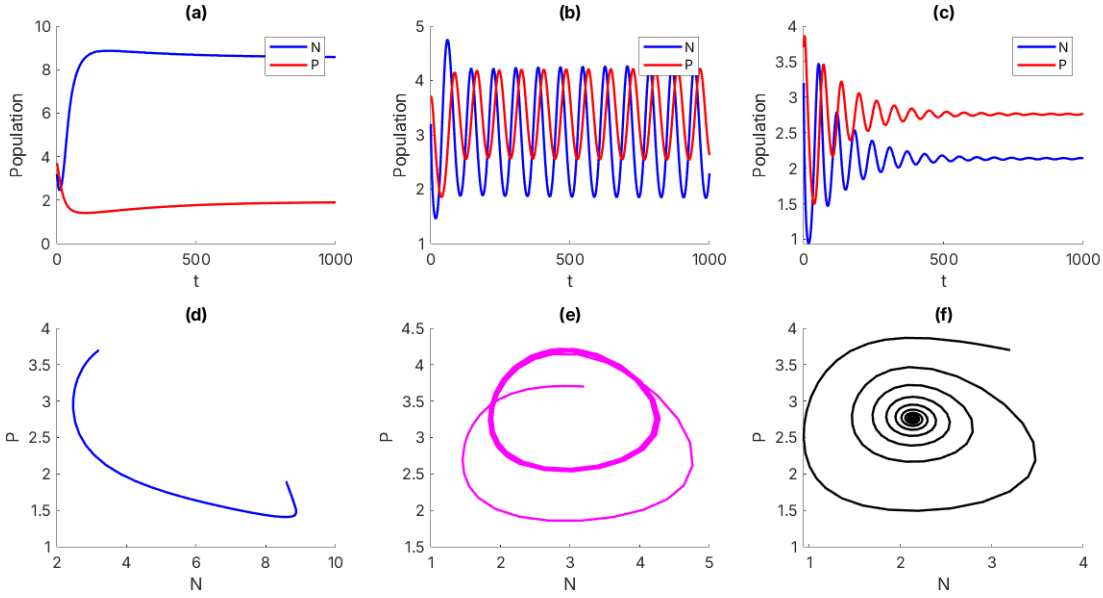


Figure 4. Time series and corresponding phase portraits of the variable carrying capacity model (2) for three values of the group defence parameter $\alpha = 0.3$ in (a) and (d); $\alpha = 0.6$ in (b) and (e); whereas $\alpha = 0.85$ in (c) and (f). All other parameters are as in Table 1.

predator-free branches lie on $P = 0$. The equilibrium branches at capacity level $\kappa = j$ are traced as the corresponding bifurcation parameter varies, with all other parameters fixed at the values in Table 1, except for the value of d_1 or q fixed in each panel as stated below.

Panel (a) shows the transcritical bifurcation of Theorem 3.9, with q as the bifurcation parameter. For $d_1 = 0.08$ we have $N^* = (d_1/ae)^{1/\alpha} \approx 2.93$, which is smaller than $N_{\text{sn}} = 4.5$, so the coexistence branch $E_{2,j}$ lies on the line $N = N^*$ and meets the lower predator-free branch $E^-_{1,j}$ at $q_{\text{TC}} = \frac{r}{E}\left(1 - \frac{N^*}{j}\right)(mE + nN^*) \approx 0.55$. The coexistence equilibrium exists for $q \le q_{\text{TC}}$ and is unstable on the plotted range. The upper branch $E^+_{1,j}$ is unstable throughout, because $ae(N'^+_j)^\alpha > d_1$ for all q shown. The branch $E^-_{1,j}$ is always unstable, since $\lambda_1 > 0$, and as q crosses q_{TC} its eigenvalue $\lambda_2 = ae(N'^-_j)^\alpha - d_1$ changes sign from negative to positive. It therefore changes from a saddle to an unstable node as the coexistence state collides with it and leaves the feasible region. This confirms the transcritical bifurcation predicted by Theorem 3.9. Because the crossing occurs on $E^-_{1,j}$, no stable state is exchanged here. A crossing on the stable part of $E^+_{1,j}$ is obtained when $N^* > N_{\text{sn}}$, as in panel (c).

Panel (b) shows the transcritical bifurcation of Theorem 3.8, with d_1 as the bifurcation parameter and $q = 0.03 < rm$, for which only the predator-free equilibrium $E^s_{1,j} = (N'^+_j, 0, j)$ exists. Since $N'^+_j \approx 9.86$ is independent of d_1, this branch remains fixed at $N = N'^+_j$. Its stability changes at $d_{1,\text{TC}} = ae(N'^+_j)^\alpha \approx 0.1658$, from a saddle for $d_1 < d_{1,\text{TC}}$ to stable for $d_1 > d_{1,\text{TC}}$. In contrast, $E_{2,j}$ varies with d_1 through $N^* = (d_1/ae)^{1/\alpha}$, which increases with d_1 and reaches N'^+_j at $d_{1,\text{TC}}$, where $P^*_j \to 0$. For $d_1 > d_{1,\text{TC}}$ we have $N^* > N'^+_j$, so $E_{2,j}$ becomes infeasible and the stable predator-free state remains. The coexistence branch is unstable for small d_1 and becomes stable as d_1 increases, before it disappears at $d_{1,\text{TC}}$. Thus, increasing predator mortality causes the coexistence state to approach the predator-free state continuously, consistent with Theorem 3.8.

Panel (c) shows the saddle-node bifurcation of Theorem 3.10, with $d_1 = 0.12$, for which $N^* \approx 5.75$ lies between $N_{\text{sn}} = 4.5$ and j. For $rm < q < q_{\text{sn}}(j)$ the predator-free equilibria $E^-_{1,j}$ and $E^+_{1,j}$ both exist. The lower branch emerges from $N = 0$ at $q = rm = 0.2$ and is unstable, and the upper branch starts at $N = j$ for $q = 0$ and decreases with q. The two branches approach each other as q increases and merge at $q = q_{\text{sn}}(j) \approx 0.6050$ at the point $N = N_{\text{sn}} = 4.5$. For $q > q_{\text{sn}}(j)$ no predator-free equilibrium exists. The upper branch $E^+_{1,j}$ is a saddle while $ae(N'^+_j)^\alpha > d_1$, and it becomes stable after the coexistence branch $E_{2,j}$ meets it in a transcritical bifurcation at $q_{\text{thresh}} = \frac{r}{E}\left(1 - \frac{N^*}{j}\right)(mE + nN^*) \approx 0.574$, which is below $q_{\text{sn}}(j)$. Beyond this point $E_{2,j}$ is infeasible. The stable $E^+_{1,j}$ then disappears together with $E^-_{1,j}$ at the saddle-node, where $\lambda_1 = 0$ and the equilibrium is non-hyperbolic, as shown in Theorem 3.6(c). Hence for $q > q_{\text{sn}}(j)$ the prey and predator densities can no longer persist at the predator-free level, which confirms the saddle-node bifurcation predicted by Theorem 3.10.

4.8. Hopf bifurcation with respect to the predator mortality rate d_1

The pointwise stability results of Section 3.3 are complemented by the bifurcation structure of system (2) as d_1 varies, with all other parameters fixed at the values in Table 1. Since $K \equiv j$ is invariant, we take $(N(0), P(0), K(0)) = (4, 2, j)$ and increase d_1 in small steps over $0.0745 \le d_1 \le 0.090$.

Figure 9 shows that for $d_1 < d_{1,H}$ the system settles onto a stable limit cycle around $E_{2,j}$. Near the left edge of the plotted range, $d_1 \approx 0.074$, the oscillations have large amplitude and the minimum of $N(t)$ approaches zero; for slightly smaller d_1, trajectories collapse to extinction, outside the plotted range. As d_1 increases, the envelope narrows and contracts to a single point at $d_{1,H} \approx 0.0804$, with a nearly vertical tangent consistent with the square-root dependence on $d_{1,H} - d_1$ expected at a Hopf bifurcation. For $d_1 > d_{1,H}$, a single branch remains, corresponding to the stable interior equilibrium $E_{2,j}$.

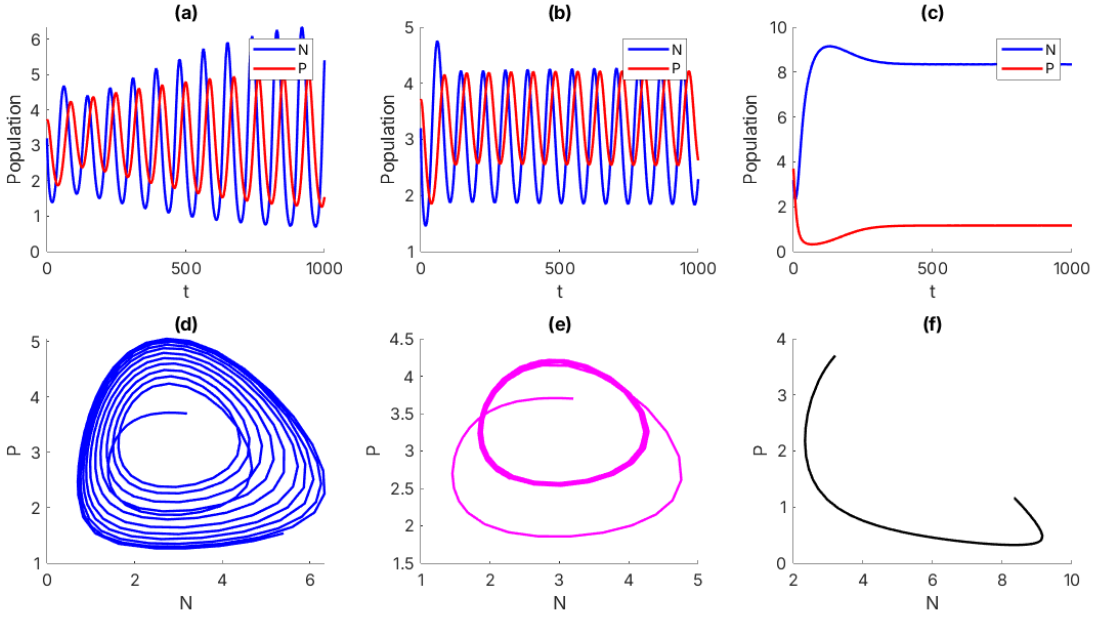


Figure 5. Time series and corresponding phase portraits of the variable carrying capacity model (2) for three values of the predator mortality rate $d_1 = 0.078$ in (a) and (d); $d_1 = 0.08$ in (b) and (e); whereas $d_1 = 0.15$ in (c) and (f). All other parameters are as in Table 1.

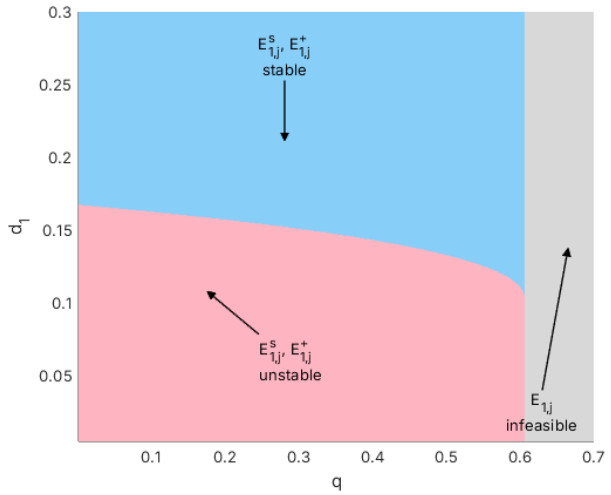


Figure 6. Feasibility and stability of the predator-free equilibria $E_{1,j}$ in the (q, d_1) plane. The grey region denotes that no predator-free equilibrium exists ($q > q_{\mathrm{sn}}(j)$). The pink region denotes $E^s_{1,j}$ ($q < rm$) or $E^+_{1,j}$ ($rm < q < q_{\mathrm{sn}}(j)$) feasible but unstable. The light blue region denotes the same equilibrium locally asymptotically stable. For $rm < q < q_{\mathrm{sn}}(j)$ the equilibrium $E^-_{1,j}$ also exists and is always unstable.

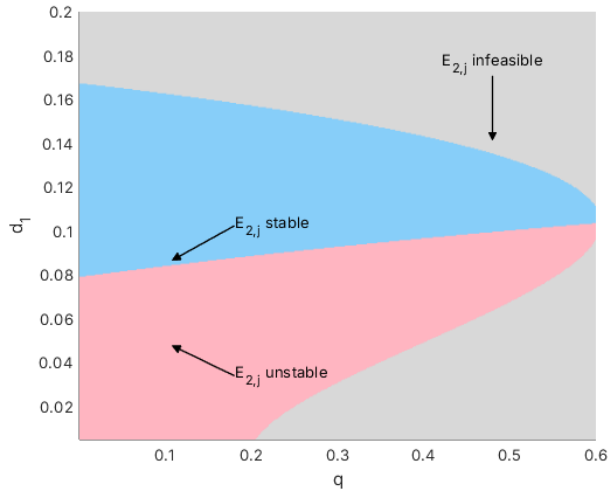


Figure 7. Feasibility and stability of the interior equilibrium $E_{2,j}$ in the (q, d_1) plane. The grey region denotes $E_{2,j}$ infeasible. The pink region denotes $E_{2,j}$ feasible but unstable ($A > 0$). The light blue region denotes $E_{2,j}$ feasible and locally asymptotically stable ($A < 0$).

At $d_1 = d_{1,H}$ we have $A = 0$ by Theorem 3.11, and numerical estimation gives $dA/dd_1|_{d_{1,H}} \approx -1.724$. The transversality condition is therefore satisfied, with A decreasing through zero as d_1 increases, consistent with the loss of oscillations beyond $d_{1,H}$.

The direction of the bifurcation is determined by the first Lyapunov coefficient. Since $K \equiv j$ is invariant and $\Gamma(j) = -\rho/(l+j) < 0$, the centre manifold lies in the plane $K = j$, so the coefficient can be computed from the planar (N, P) subsystem. The parameters of Table 1, gives $a_1 \approx -1.67 \times 10^{-4} < 0$. Together with $dA/dd_1|_{d_{1,H}} < 0$, this shows that the Hopf bifurcation is supercritical.

4.9. Verification of explicit recovery-time law

Equation (9) was verified numerically for $l \in \{0.5, 1, 5, 10, 50\}$ and $\eta \in \{0.5, 0.9\}$, with $i = 1$, $j = 10$, $\rho = 0.5$ and $K_0 = 1.45$. The recovery times obtained by integrating equation (1) agree with the closed-form values to within 10^{-8}. Figure 10(a) shows that T_η increases strictly with l, as established in Theorem 3.13. It is in fact linear in l, with slope $\frac{1}{\rho}\left[\ln\frac{\eta(j-i)}{K_0-i} - \ln\frac{(1-\eta)(j-i)}{j-K_0}\right] > 0$. Panel (b) shows the corresponding delay in the approach of $K(t)$

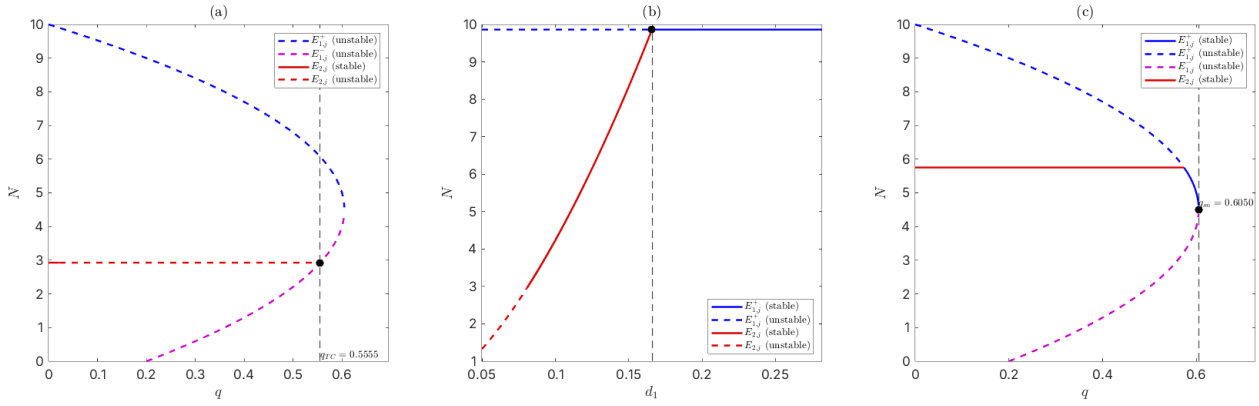


Figure 8. Bifurcations of system (2), showing N at $\kappa = j$. Panel (a) shows the transcritical bifurcation in q at $q_{\mathrm{TC}} = 0.55$, with $d_1 = 0.08$. Panel (b) shows the transcritical bifurcation in d_1 at $d_{1,\mathrm{TC}} = ae(N_j'^{+})^{\alpha} = 0.1658$, with $q = 0.03$. Panel (c) shows the saddle-node bifurcation in q at $q_{\mathrm{sn}}(j) = 0.605$, with $d_1 = 0.12$. Solid curves denote locally asymptotically stable branches, dashed curves denote unstable branches, and filled circles mark the bifurcation points. Vertical dashed lines mark the bifurcation values.

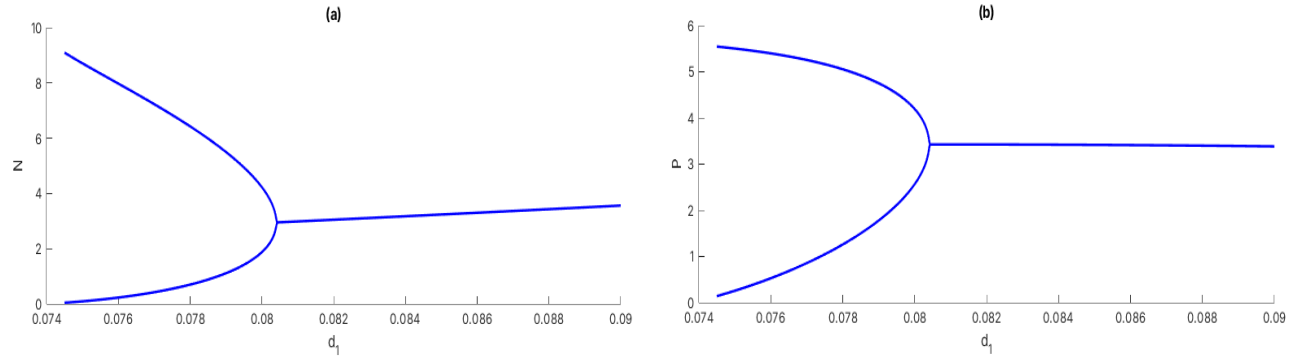


Figure 9. Bifurcation diagram of system (2) with respect to the predator mortality rate d_1, holding all other parameters at the values in Table 1. Panel (a) shows the envelope of $N(t)$ and panel (b) the envelope of $P(t)$, given by the minimum and maximum over a recording window after a long discarded transient, with d_1 increased in small steps from 0.0745. The upper and lower branches merge continuously at the Hopf threshold $d_{1,H} \approx 0.0804$ of Theorem 3.11.

to j as l increases. Since the carrying-capacity equation does not depend on N or P, l and K_0 affect only the time needed for K to recover. The asymptotic predator–prey dynamics are those of the constant-K model with $k = j$.

5. Discussion

This study advances predator–prey theory by coupling a population system featuring prey group defence and non-linear Michaelis–Menten harvesting with a dynamically evolving environmental carrying capacity. Whereas classical ecological models treat carrying capacity as static and standard dynamic extensions assume a constant per-capita adjustment rate, the primary novelty of our formulation lies in a saturating modification of the shifted-logistic law. This mechanism constrains the habitat between a strictly positive minimum floor and an upper sustainable ceiling while forcing the per-capita rate of environmental recovery to saturate as resource availability grows. As this saturating law reduces asymptotically to the classical shifted-logistic form when the saturation threshold is large, it bridges constant-rate and resource-limited recovery within a single analytical framework. Crucially, the formulation admits an exact implicit solution and a closed-form expression for the time required to recover to any prescribed intermediate capacity level, proving analytically that stronger saturation strictly lengthens habitat recovery times whereas a higher maximal adjustment rate shortens them.

The structural coupling between the regenerating environment and the trophic interaction yields a comprehensive picture of both boundary and interior population dynamics. Because the carrying capacity evolves independently of the populations, the governing system possesses a block-triangular structure in which the lower capacity boundary is universally repelling; consequently, all equilibria associated with the minimum capacity are unstable, and long-term persistence is possible only at the upper capacity ceiling. At this restored level, our analysis provides a complete classification of the predator-free equilibria, demonstrating that non-linear harvesting can induce multiple boundary states that merge and vanish through a saddle-node bifurcation once harvesting pressure exceeds a critical threshold. The transition between predator-free persistence and species coexistence is governed by two distinct transcritical bifurcations driven by harvesting catchability and predator mortality, while the interior coexistence state undergoes a supercritical Hopf bifurcation that generates stable limit cycles. Within the coexistence regime, the model reveals a sharp contrast between trophic parameters: predator mortality acts monotonically as a stabilising mechanism

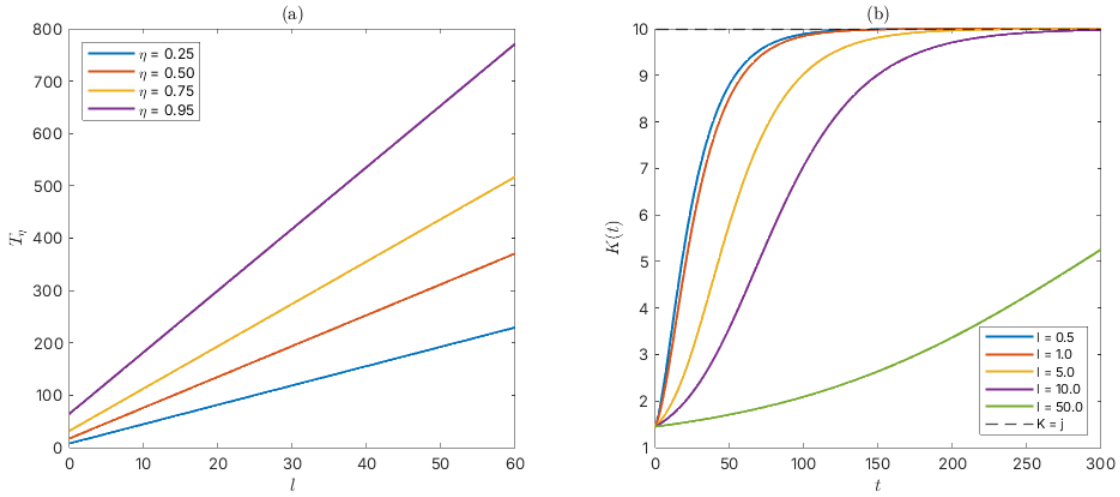


Figure 10. Verification of the explicit recovery-time law in Theorem 3.12 and its monotonicity in l (Theorem 3.13), with $i = 1$, $j = 10$, $\rho = 0.5$, and $K_0 = 1.45$. Panel (a) shows the closed-form recovery time T_η as a function of l for four values of η. Panel (b) shows the corresponding exact trajectories $K(t)$ obtained by numerically inverting equation (8); the dashed line denotes the equilibrium $K = j$.

that dampens oscillations, whereas prey group defence exerts a non-monotonic influence, inducing sustained oscillations at intermediate defensive strengths while maintaining stable coexistence at both weak and strong levels of group defence.

The overarching contribution of this work is the analytical separation of transient environmental restoration from asymptotic population behaviour. The speed and trajectory of habitat recovery govern how long the populations remain in a vulnerable transient regime, whereas the ultimate ecological outcome—whether predator extinction, stable coexistence, or periodic oscillation—is dictated entirely by the upper capacity limit and the demographic parameters. Notably, the local departure rate from the lower capacity boundary decreases as the minimum capacity floor rises, revealing that an environment with a higher baseline reserve can experience a more prolonged initial recovery plateau despite starting closer to its equilibrium ceiling. This framework therefore provides a rigorous, quantitative tool for evaluating how long a depleted ecosystem takes to return to its sustainable state without distorting the long-term predictions of the underlying predator–prey interaction, noting that historical capacity trajectories could alter the final population state only if the limiting trophic system admitted multiple coexisting attractors.

Two limitations of the present study should be noted as directions for future work. First, the carrying capacity evolves autonomously and receives no feedback from the prey or predator populations, meaning that consumer-driven habitat degradation such as overgrazing and positive trophic feedbacks on resource regeneration are not captured. Second, the bifurcation and stability results are local in character and are illustrated using representative parameter regimes rather than calibrated to empirical field measurements, leaving the global stability of the coexistence state, the uniqueness of limit cycles away from the Hopf threshold, and system-specific ecological forecasting as open problems for further investigation.

Declarations

Acknowledgements: The authors like to acknowledge the learned rivewer for their constructive advise which helps the manuscript to take a good shape and enriched its scientific values.

Funding: None of the authors got funding from any organisations for this work.

Data availability Statement: No data associated in the manuscript.

Conflict of interest: Authors declare that they have no conflicts of interest.

Ethical approval: This article does not contain any with human participants or animal performed by any of the authors.

Use of AI Tools: No AI tools were used to prepare this manuscript.

Author Contributions: BB develope the mathematical models, analyse both analytical and numerical parts, and write the manuscript. PND conceptualise the problem, revise the manuscrip, and supervise the work.

REFERENCES

[1] M. H. Carr, T. W. Anderson, and M. A. Hixon, Biodiversity, population regulation, and the stability of coral-reef fish communities, *Proceedings of the National Academy of Sciences*, vol. 99, no. 17, pp. 11241–11245, 2002. doi:10.1073/pnas.162653499.

[2] M. A. Hixon and M. H. Carr, Synergistic predation, density dependence, and population regulation in marine fish, *Science*, vol. 277, no. 5328, pp. 946–949, 1997.

[3] R. Dawkins and J. R. Krebs, Arms races between and within species, *Proceedings of the Royal Society of London. Series B*, vol. 205, no. 1161, pp. 489–511, 1979.

[4] A. J. Lotka, *Elements of Physical Biology*. Baltimore: Williams and Wilkins, 1925.

[5] V. Volterra, Fluctuations in the abundance of a species

considered mathematically, *Nature*, vol. 118, pp. 558–560, 1926. doi:10.1038/118558a0.

[6] Z. Tablado, P. Fauchald, G. Mabille, A. Stien, and T. Tveraa, Environmental variation as a driver of predator–prey interactions, *Ecosphere*, vol. 5, no. 12, art. 164, 2014. doi:10.1890/ES14-00121.1.

[7] S. Sarwardi, P. K. Mandal, and S. Ray, Dynamical behaviour of a two-predator model with prey refuge, *Journal of Biological Physics*, vol. 39, no. 4, pp. 701–722, 2013. doi:10.1007/s10867-013-9327-7.

[8] M. Mukherjee, D. Pal, S. K. Mahato, and E. Bonyah, Prey–predator optimal harvesting mathematical model in the presence of toxic prey under interval uncertainty, *Scientific African*, vol. 21, art. e01837, 2023. doi:10.1016/j.sciaf.2023.e01837.

[9] G. M. McKeon, G. S. Stone, J. I. Syktus, J. O. Carter, N. R. Flood, D. G. Ahrens, D. N. Bruget, C. R. Chilcott, D. H. Cobon, R. A. Cowley, S. J. Crimp, G. W. Fraser, S. M. Howden, P. W. Johnston, J. G. Ryan, C. J. Stokes, and K. A. Day, Climate change impacts on northern Australian rangeland livestock carrying capacity: A review of issues, *The Rangeland Journal*, vol. 31, no. 1, pp. 1–29, 2009. doi:10.1071/RJ08068.

[10] E. Calizza, M. L. Costantini, G. Careddu, and L. Rossi, Effect of habitat degradation on competition, carrying capacity, and species assemblage stability, *Ecology and Evolution*, vol. 7, no. 15, pp. 5784–5796, 2017. doi:10.1002/ece3.2977.

[11] J. J. Shepherd and L. Stojkov, The logistic population model with slowly varying carrying capacity, *ANZIAM Journal*, vol. 47, pp. C492–C506, 2005.

[12] P. S. Meyer and J. H. Ausubel, Carrying capacity: A model with logistically varying limits, *Technological Forecasting and Social Change*, vol. 61, no. 3, pp. 209–214, 1999.

[13] S. Kumar and H. Kharbanda, Chaotic behavior of predator-prey model with group defense and non-linear harvesting in prey, *Chaos, Solitons and Fractals*, Elsevier, 2019.

[14] Chaoqun Xu, Sanling Yuan, and Tonghua Zhang, Global dynamics of a predator–prey model with defense mechanism for prey, *Applied Mathematics Letters*, vol. 62, pp. 42–48, 2016, doi: 10.1016/j.aml.2016.06.013.

[15] L. Perko, *Differential Equations and Dynamical Systems*, 3rd ed. New York: Springer-Verlag, 2001.